The Contribution of Dutch GLOBE Schools to Validation of Aerosol Measurements from Space

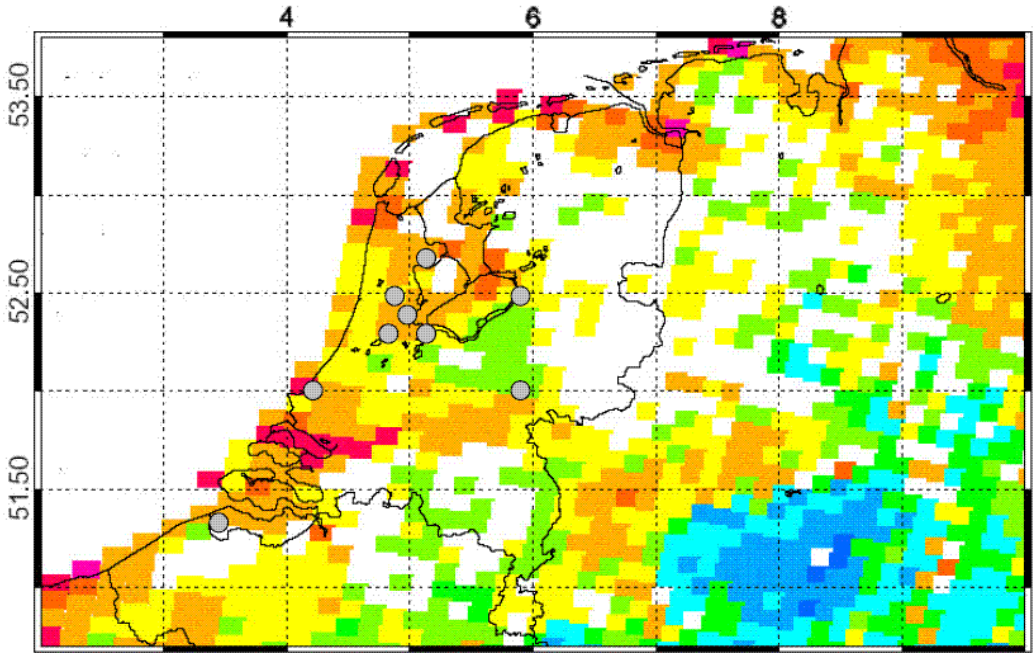

Joris de Vroom
Vrije Universiteit Amsterdam
October 2003

vrije Universiteit amsterdam

KNMI

OMI

Index

List of Acronyms

AERONET	Aerosol Robotic Network
AOT	Aerosol Optical Thickness
BBL	Beer -Bougeur-Lambert
FEL	Fysisch en Electrisch Laboratorium (Physics and Electronics Laboratory)
GLOBE	Global Learning and Observations to Benefit the Environment
GOME	Global Ozone Monitoring Experiment
IR	Infra-Red
KNMI	Koninklijk Nederlands Meteorologisch Instituut (Royal Dutch Meteorological Institute)
LED	Light Emitting Diode
LUT	Look Up Table
MODIS	Moderate Resolution Imaging Spectroradiometer
NASA	National Aeronautics and Space Administration
OMI	Ozone Monitoring Instrument
PI	Principle Investigator
SCIAMACHY	Scanning Imaging Absorption Spectrometer for Atmospheric Chartography
SME	Stichting Milieu Educatie (Foundation for Environmental Education)
SPUV	Sun Photometer Ultra Violet
TNO	Nederlandse Organisatie voor Toegepast Natuurwetenschappelijk onderzoek (Netherlands Organization for Applied Scientific Research)
TPD	Technische Physische Dienst (Technical Physical Service)
UT	Universal Time
VIS	Visible

1 Introduction

In the past century, the mean surface temperature of the Earth has increased by 0.6˚ according to the International Panel of Climate Change [*IPCC*, 2001]. Figure 1.1 shows the mean Earth's surface temperature since 1860. The red bars are the mean annual temperature deviation from the 1961 – 1990 average and the red line is a 10 year average. The black line in Figure 1.1 shows a distinct trend upward. Since the industrial revolution, large-scale industrious human activities have accounted for an increase in greenhouse gas concentrations in the atmosphere. Greenhouse gases like carbon dioxide (CO_2) and methane (CH_4) absorb infrared radiation, thereby influencing the radiation balance and warming the Earth. Furthermore, human activities have accounted for a large increase in small solid or liquid atmospheric particles, called aerosols.

The effect of aerosols on the radiation budget is complicated. Figure 1.2 [*IPCC*, 2001] shows the level of understanding of the radiative effects, called radiative forcing, resulting from an increase in aerosol and greenhouse gas concentrations [*IPCC*, 2001]. The radiative forcing caused by aerosols is still very poorly understood, but might even be as large (but negative) as the radiative forcing caused by greenhouse gasses. The first mechanism by which aerosols influence our climate system is by reflecting and absorbing Solar radiation and infrared thermal radiation from the Earth's surface. This is called the aerosol direct effect. Some aerosol species, like for example black carbon, absorb radiation at long wavelength, thus warming the Earth's climate system. Other species, like for example desert dust, effectively scatter Solar radiation, thus increasing the planetary albedo and cooling the Earth's climate system. Aerosol direct forcing is currently considered to give a cooling effect [*Kaufman et al*, 2001], although some aerosol types, like black carbon, may give a warming effect. The second mechanism by which aerosols influence our climate system is by using as condensation nuclei for water vapor, thereby enhancing the process of cloud forming, resulting in more clouds. Furthermore, these clouds consist of more cloud droplets, which are smaller in size. This increases both the reflectivity and lifetime of clouds. This is called aerosol indirect effect. Clouds reflect Solar radiation, giving a cooling effect, and they reflect infrared radiation from the Earth's surface, giving a warming effect. The net effect of the aerosol indirect effect is currently considered to be cooling the Earth's surface [*Kaufman et al.,* 2002]. The effects of aerosols in our climate system described above illustrate the need to monitor aerosols. Besides the effect on climate, other reasons for the need to monitor aerosols are that high aerosol concentrations in urban regions can cause smog, which may lead to human health problems, and that aerosols affect the chemical composition of the atmosphere by the alteration of photolysis rates and by direct chemical interaction with gasses [*Kaufman et al*, 2002].

Aerosols can be grouped into five categories: dustlike soil, soot, sulfate, sea salt and organic aerosols [*Liou*, 2002]. Dustlike soil and sea salt aerosol particles have a typical diameter larger than 1 μm while soot, sulfate and organic aerosol have a typical diameter smaller than 1 μm. Aerosol concentrations are highly variable in space and time, caused by the relatively short lifetime of an aerosol particle, and the differences in aerosol sources. Examples of aerosols sources are forest fires, human industrial activities and sand storms. Furthermore, it is difficult to distinguish anthropogenic aerosols from natural aerosols. Except for marine aerosol, all types of aerosols can have both natural and anthropogenic sources. However, it is possible to estimate the anthropogenic contribution to the total aerosol load using satellite data, aerosol models and information on fire practices and agricultural and industrial activities.

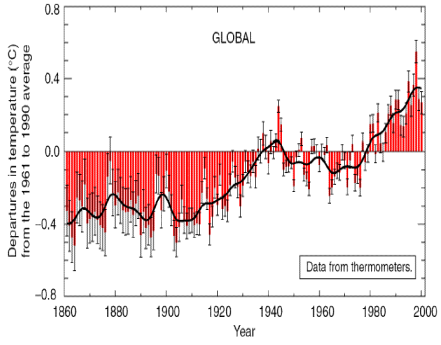

Figure 1.1. Variations of the earth's surface temperature for the past 140 years, deviation from the 1961 – 1990 average. Figure adopted from *IPCC*, 2001.

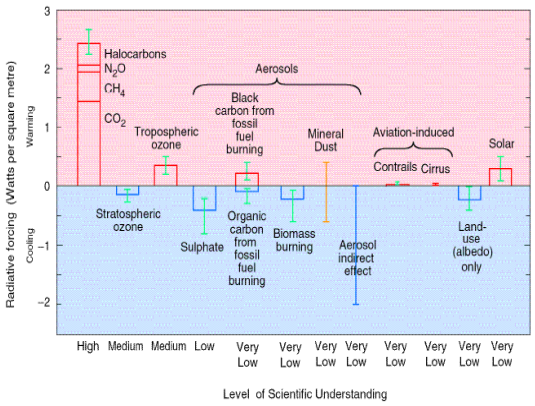

Figure 1.2. The global mean radiative forcing of the climate system for the year 2000 relative to 1750. Figure adopted from *IPCC*, 2001.

Since aerosols influence the climate system of the Earth and since there are still large uncertainties about their radiative effects it is necessary to monitor aerosols. This is done on a local basis by solar radiance measurements with Sun photometers, which measure the light extinguished by aerosols, expressed in aerosol optical thickness (AOT). These Sun photometers have the advantage that they are able to produce continuous AOT time series with high accuracy. However, such time series are valid only for the fixed measuring location. A network of Sun photometers is the Aerosol Robotic Network (AERONET), with over a hundred Sun photometers, stationed all over the world. AOT measurements between various AERONET instruments on different locations show large differences. Therefore, measurements on a global scale are essential. A way to measure AOT on a global scale is by using satellite instrument measurements. An advantage of satellite instrument measurements is that global coverage can be achieved within a few days. However, difficulties with satellite measurements may be expected due to instrument degradation in the harsh outer space environment and the fact that the instrument cannot be approached after launch. Therefore it is essential that the accuracy and precision of satellite instrument measurements are checked by comparisons to ground-based measurements throughout the entire satellite mission. This is called validation. In order to achieve a high accuracy of validation, it is desirable to validate as many satellite ground pixels as possible. Validation with expensive, professional Sun photometers is limited to a relatively small amount of ground pixels for satellite instruments with a spatial resolution of 13 x 24 km^2, such as the Ozone Monitoring Instrument (OMI) (Figures 1.3 and 1.4). The contribution of the GLOBE Aerosol Monitoring Project to satellite validation is investigated in this report. The GLOBE Aerosol Monitoring Project has the potential to supply a tight network of ground-based AOT measurements that can validate many satellite pixels over land, thereby improving satellite validation.

The GLOBE Aerosol Monitoring Project

The GLOBE (Global Learning and Observations to Benefit the Environment) program is an international science and education program. It started in 1995 by initiative of Al Gore, the then vice-president of the United States, and is currently running in 102 countries. GLOBE is a partnership between the United States and the 102 other countries. The goal of the GLOBE program is involving primary and secondary school students in practical science by taking scientifically valid measurements.

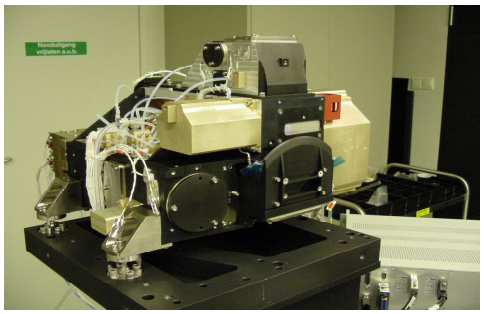

Figure 1.3. The Ozone Monitoring Instrument, autumn 2001, at the beginning of testing period at TNO-TPD. Picture by TNO-TPD.

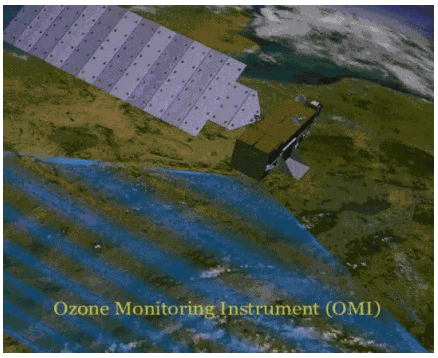

Figure 1.4. OMI on EOS-AURA (artist impression).

The GLOBE Aerosol Monitoring Project is coordinated by David Brooks, from the Drexel University in Philadelphia. The project involves validation of satellite AOT measurements with AOT measurements by undergraduate students using a handheld Sun photometer, developed for the GLOBE program [*Brooks and Mims,* 2001]. The Dutch division of GLOBE is represented by GLOBE Netherlands. Over a hundred schools are involved in cloud observations, phenology and measuring meteorological parameters, acidification and aerosols. The Dutch GLOBE Aerosol Monitoring Project is a co-operation between SME (Foundation for Environmental Education) and KNMI (Royal Dutch Meteorological Institution). SME accounts for the organization and contact with schools and KNMI is responsible for data processing, quality control and satellite validation. KNMI has experience in satellite validation with the satellite instrument GOME (Global Ozone Monitoring Experiment). Furthermore, KNMI is Principle Investigator (PI) for the validation of the Dutch-German-Belgium satellite instrument SCIAMACHY (Scanning Imaging Absorption Spectrometer for Atmospheric Chartography) and is PI for OMI. The goals of the Dutch GLOBE Aerosol Monitoring Project for KNMI are threefold:

1. Validation of satellite aerosol optical thickness measurements.
2. Public outreach for Dutch satellite instrument missions such as SCIAMACHY and OMI.
3. Involve students in practical science.

To illustrate the potential of the GLOBE Aerosol Monitoring Project, AOT measurements at 440 nm by the satellite instrument MODIS (Moderate Resolution Imaging Spectroradiometer) from April 8 2003 at 10:00 UT (Universal Time) are plotted in Figure 1.5. The white areas indicate regions without a reliable MODIS measurement, for example over sea or clouds. The two black dots in Figure 1.5 represent the two professional Sun photometers in the Netherlands at TNO-FEL (Netherlands Organization for Applied Scientific Research - Physics and Electronics Laboratory) in The Hague and at KNMI in De Bilt. The grey dots represent schools that currently participate in the GLOBE Aerosol Monitoring Project. Table 1.1 shows the names of the nine schools and their location. Figure 1.5 shows that the Dutch GLOBE school network improves the potential of validating satellite measurements over the Netherlands. Since nine schools are interested in joining the GLOBE training in September 2003 at KNMI, the number of schools is expected to get larger. The “Bernard Nieuwentijt college”, “Pascal college”, “Alkwin college”, “SG. Tabor” and “Goois lyceum” are urban regions, in or close to Amsterdam. “Christelijk college De Populier” and “Zwin” college are located at a very interresting locations, since they are both coastal regions and relatively close to Rotterdam (51.7° N, 4.2° E) which is a very industrious area, and various types of aerosol may be expected at different wind directions. Furthermore ‘‘De Populier’’ is close to the AERONET instrument at TNO-FEL in The Hague. The “Mozaiek” college and “Ichthus” college are located at less industrious regions. The region around Amsterdam shows relatively good coverage. SME is looking for more schools in the East, South-East and North-East to generate a more homogeneous coverage over the Netherlands.

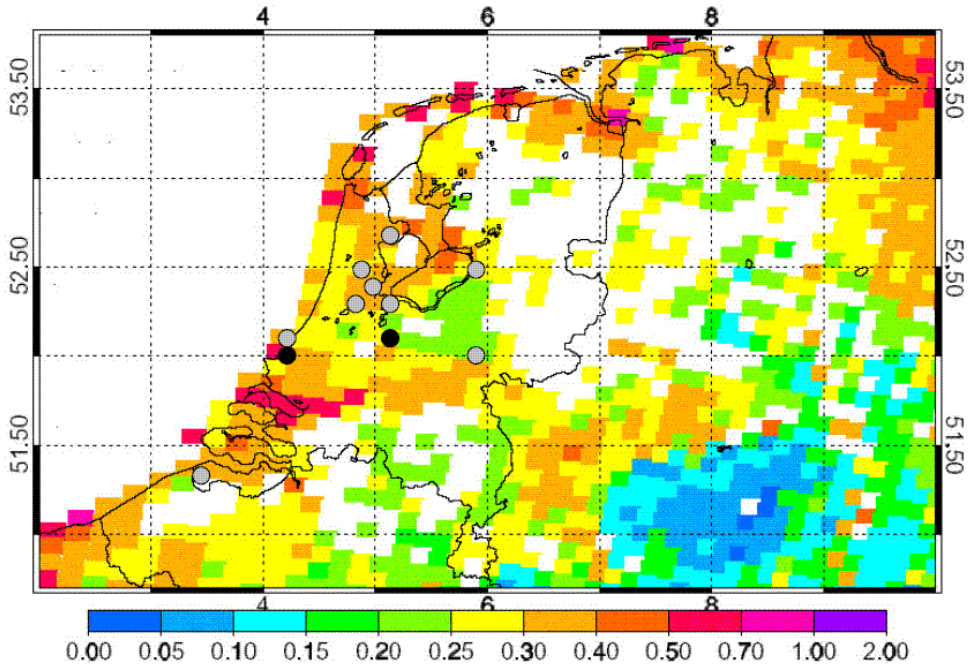

Figure 1.5. GLOBE potential for satellite validation. MODIS AOT at 440 nm over the Netherlands on 2003-04-08

School name	School location	Latitude (North)	Longitude (East)	Participating Since
Bernard Nieuwentijt College	Amsterdam	52.38°	4.93°	01-2002
Pascal College	Zaandam	52.46°	4.83°	01-2002
Christelijk Collgede de Populier	The Hague	52.05°	4.16°	01-2002
Mozaiek College	Arnhem	51.98°	5.92°	01-2002
Alkwin College	Uithoorn	52.25°	4.82°	03-2003
SG. Tabor, Locatie Oscar Romero	Hoorn	52.70°	5.10°	03-2003
Goois Lyceum	Bussum	52.16°	5.10°	03-2003
Zwin College	Oostburg	51.32°	3.49°	03-2003
Ichthus College	Kampen	52.50°	5.90°	03-2003

Table 1.1. Participating schools and locations.

In reference to aerosols and its role in the climate system, the need to measure aerosol with satellite measurements and the potential of the Dutch GLOBE Aerosol Monitoring school network, the main questions that is to be answered in this paper is:
Can the Dutch GLOBE school network be used to validate satellite instruments?
In order to answer this question, the following sub questions are formulated and answered in this paper:

1. Can GLOBE Sun photometer measurements be used for validation in a theoretical way? This is answered by looking at the instrument and its measuring method, development of an algorithm and analysis of error sources.

2. Can GLOBE Sun photometer measurements be used for validation in a practical way? This is answered by comparing GLOBE Sun photometer measurements done at KNMI with measurements by a professional Sun photometer.
3. Can GLOBE Sun photometer measurements by undergraduates be used for validation? This is answered by comparing Sun photometer measurements done by undergraduates with measurements by a professional Sun photometer.

Finally, the results are applied to validation of MODIS AOT measurements over the Netherlands by the Dutch GLOBE aerosol monitoring school network.

2 GLOBE Sun photometer measurements

The GLOBE Aerosol Monitoring Project involves aerosol optical thickness (AOT) measurements with light emitting diode (LED)-based GLOBE Sun photometers by undergraduate students. The use of a LED as a detector is what distinguishes the GLOBE Sun photometer from professional Sun photometers. The relatively wide spectral response of the LED effects the interpretation of results from GLOBE Sun photometer measurements. The purpose of this chapter is to investigate the possibility of accurately measuring AOT with the GLOBE Sun photometer. The GLOBE Sun photometer instrument is described in section 2.1. The physical principle that underlies the measuring method is the Beer-Bougeur-Lambert (BBL) law, which is introduced in section 2.2. The measuring method of the GLOBE Sun photometer is discussed in section 2.3. Assumptions with respect to relative air mass calculations and an equation for the relative air mass are discussed in section 2.4.1 Assumptions with respect to the relatively wide spectral response of the LEDs are discussed in section 2.4.2. The conclusions are presented in section 2.5.

2.1 Instrument description

In the GLOBE Aerosol Monitoring Project, direct Solar measurements are done with the LED-based Sun photometer developed for the GLOBE project, as first described by *Mims* [1992]. The instrument is schematically pictured in Figure 2.1. Two LEDs are used as light detectors, one at 508 nm (green), and one at 625 nm (red). A 9 Volt battery is present to supply power to the LEDs. When a beam of light shines on a LED, a current proportional to the light intensity is produced [*Mims,* 1992]. The current is sent through a resistance and the voltage over the resistance is measured with a voltmeter. The LEDs have a response bandwith of approximately 75 nm (green) and 40 nm (red). The 508 and 625 nm values are effective wavelengths. The concept of effective wavelengths will be discussed in section 2.4.2.

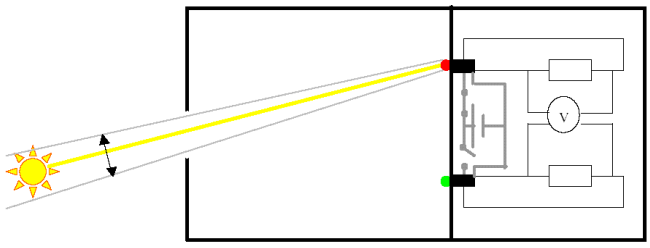

Figure 2.1. LED-based Sun photometer for the GLOBE project. The detector's opening angle is exaggerated for illustrative reasons. The rectangles with the green and red spheres represent the LEDs.

The use of a LED as a detector is what distinguishes the GLOBE Sun photometer from professional Sun photometers. Advantages of using LEDs are that they are widely available, inexpensive and have stable optical properties. A disadvantage is that their spectral response bandwith is large (up to 75 nm). The implication of this is discussed in section 2.4.2. Professional instruments, on the other hand, use detectors with a spectral response of about 15 nm and they are available in a wide range of wavelengths, but they are expensive and delicate. The cheap GLOBE Sun photometer is therefore very useful for the GLOBE Aerosol Monitoring Project, in which the instrument is used in large numbers. In addition, the robustness of the GLOBE Sun photometer is an advantage since it is used by undergraduate students who cannot be expected to handle the instrument with the same care as experienced scientists.

There is an essential difference between the measuring methods of measurements done with professional Sun photometers and measurements done with the GLOBE Sun photometer. A professional Sun photometer is usually placed on an automatic Suntracker which makes it possible to automatically measure AOT with a small, constant sample time during the whole day. A GLOBE Sun photometer measurement requires the physical presence of students, who have to align the instrument every measurement, which introduces a measuring uncertainty because of small alignment errors. On the other hand, their physical presence allows the registering of metadata like aircraft contrails in the light path, cloud cover and haze at the time of measurement, thus providing valuable additional information that professional instrument sometimes lack.

2.2 Physical principles

The amount of light extinguished by aerosols is determined by both the total aerosol column between the detector and the Sun, and the aerosol absorption and scattering characteristics. In principle, no a priori knowledge about the aerosol type prevailing over the measurement location is available. Since the absorption and scattering characteristics depend on the aerosol type, assumptions on aerosol type have to be made in order to retrieve the total aerosol column. To avoid such assumptions, the total aerosol load in the atmosphere is usually represented by AOT. This dimensionless number represents the light extinction caused by scattering and absorption by aerosols along the light path. The advantage of representing aerosol by AOT instead of the aerosol column is that it is possible to directly compare measurements done at different times and locations without assumptions on aerosol type.

When AOT is measured at two wavelengths or more it is possible to retrieve information on aerosol particle size. Scattering and absorption by aerosols usually shows a wavelength dependence according to the empirical relation found by *Ångström* [1929], which states that AOT (τ_a) decreases with wavelength (λ) as follows,

$$\tau_a(\lambda) = \tau_a(\lambda_0)\left(\frac{\lambda}{\lambda_0}\right)^{-\alpha}, \tag{2.1}$$

where α is the so called Ångström coefficient that ranges between 0 and 2.5. For example, the mean value of α is 1.398 at De Bilt *[Stammes and Henzing*, 2000]. The exact value of α depends on the aerosol particle size distribution. Large aerosol particles (< 1μm), like sea salt and soil dust, generally give rise to a small value for α, while small aerosol particles (> 1μm), like soot and sulfates, generally give rise to large values for α. From the AOT of two different wavelengths, that are not too close, α can be determined and information on particle size distribution can be retrieved.

The measuring method of a Sun photometer is based on the Beer-Bouguer-Lambert (BBL) law. The BBL law states that the intensity of a monochromatic beam of Sunlight, $I(\lambda)$, at the detector is,

$$I(\lambda) = I_0(\lambda)e^{-\tau(\lambda)M(t)}, \tag{2.2}$$

with $I_0(\lambda)$ the Solar irradiance at wavelength λ at the top of the atmosphere (TOA), $\tau(\lambda)$ the optical thickness of the atmosphere at wavelength λ and $M(t)$ the relative air mass, that can be interpreted as the light path through the atmosphere and is 1 for overhead Sun (at the Earth's surface at sea level). In Eq. 2.2 it is assumed that the intensity of scattered light at the detector is negligible which is a realistic assumption considering that if the instrument is aligned right next to the Sun the response is zero. If we assume that the instrument gives a response voltage that is proportional to the incoming light intensity at λ, we can replace $I(\lambda)$ and $I_0(\lambda)$ in Eq. 2.2 by $V(\lambda)$ and $V_{0,\lambda}$ respectively. $V_{0,\lambda}$ then represents the voltage the instrument would measure at the top of the atmosphere. The value of $V_{0,\lambda}$ depends on the instrument's characteristics and is called the extraterrestrial constant of the instrument. Since it is an instrument constant the λ-dependence is dropped, but in general, $V_{0,\lambda}$ is not equal for the two channels (508 nm and 625 nm) and that is why λ appears as an index. $V_{0,\lambda}$ is multiplied by $(r_0/r(t))^2$, where $r(t)$ is the Earth-Sun distance and r_0 is one Astronomical Unit (AU), in order to account for the variations in TOA radiance due to the seasonal variation in the Earth-Sun distance. We write $r_0/r(t)$ explicitly to illustrate that r is a function of time. The equation relating the instrument's voltage to the optical thickness of the atmosphere then becomes,

$$V(\lambda) = \left(\frac{r_0}{r(t)}\right)^2 V_{0,\lambda}e^{-\tau(\lambda)M(t)}. \tag{2.3}$$

In principle, $V_{0,\lambda}$ also varies in time because of fluctuations of $I_{0,\lambda}$ due to variations in number of sunspots but this effect is smaller than 0.2 % [*Liou*, 2002] and therefore neglected.

The total optical thickness of the atmosphere, $\tau(\lambda)$, is the sum of Rayleigh scattering optical thickness, $\tau_R(\lambda)$, optical thickness due to absorption by gases, $\tau_g(\lambda)$, and optical thickness due to scattering and absorption by aerosols, $\tau_a(\lambda)$. If $\tau(\lambda)$ is known and Rayleigh scattering and absorption by gases can be corrected for, $\tau_a(\lambda)$ can be retrieved. In order to calculate $\tau(\lambda)$ and consequently $\tau_a(\lambda)$ from Eq. 2.3, knowledge of $V(\lambda)$, $V_{0,\lambda}$ and $M(t)$ is required. $V(\lambda)$ is the actual measurement. The determination of $V_{0,\lambda}$ is discussed in the next chapter and the calculation of $M(t)$ from the Solar elevation angle is discussed in section 2.4.1.

Apart from Rayleigh scattering, absorption by gases and absorption and scattering by aerosols, there is also scattering and absorption by clouds when present. In practice it is impossible to distinguish the light extinction due to aerosols from the light extinction by clouds. Therefore, AOT retrieval is possible only when the Sun is not obscured by clouds. Recognising cloud-free conditions and correctly reporting cloud conditions is therefore essential for reliable AOT retrieval.

2.3 Measurement method

In order to retrieve $\tau_a(\lambda)$ from Eq. 2.3 we need to know $V_{0,\lambda}$. This can be done with the Langley method [*Liou*, 2002]. The idea of the Langley method is to measure $V(\lambda)$ for a wide range of relative air masses (or Solar zenith angles). A plot of $\ln(V(\lambda))$ versus $M(t)$ may be extrapolated to the zero point, which represents the top of the atmosphere ($M(t) = 0$). This method has the advantage of being easy, relative to measuring $I_{0,\lambda}$ at the top of the atmosphere. Taking the logarithm on both sides of Eq. 2.3 it is clear that, if the BBL law can be applied, the Langley plot should be a straight line,

$$\ln(V(\lambda)) = \ln\left(\left(\frac{r_0}{r(t)}\right)^2 V_{0,\lambda}\right) - \tau(\lambda)M(t). \tag{2.4}$$

The slope of the Langley plot is $\tau(\lambda)$, the total (time-averaged) optical thickness of the atmosphere and the zero point ($M(t) = 0$) is $\ln((r_0/r)V_{0,\lambda})$. For an accurate determination of $V_{0,\lambda}$ the optical thickness of the atmosphere should be constant during the day of measurement. This condition can be satisfied by taking the Langley plot measurements on a clear day with constant (and therefore preferably low) AOT. Furthermore the Langley plot method is only valid if the BBL law holds, that is if the instrument detects a monochromatic beam of light. Since all instruments detect over a finite bandwith this is an approximation that should be investigated. The validity of the Langley plot method for the 75 nm broadband LED-based Sun photometer is discussed in section 2.4.2.

If a particular Sun photometer's extraterrestrial constant $V_{0,\lambda}$ is known, other instruments can be calibrated by determining response ratios to the calibrated instrument, which is used as a reference instrument. Response ratios are determined by comparing simultaneous measurements of the reference instrument and the instrument under calibration. This method saves the time-consuming Langley plot measurements for every individual instrument and is very useful for the GLOBE Aerosol Monitoring Project, in which 20 GLOBE Sun photometers are in use.

When $V_{0,\lambda}$ is known, we obtain the equation for the optical thickness of the atmosphere $\tau(\lambda)$ by rearranging terms in (Eq. 2.4)

$$\tau(\lambda) = \frac{1}{M(t)} \ln\left(\frac{\left(\frac{r_0}{r(t)}\right)^2 V_{0,\lambda}}{V(\lambda)}\right). \tag{2.5}$$

In order to determine the contribution $\tau_a(\lambda)$ to the total optical thickness, $\tau(\lambda)$, we subtract Rayleigh optical thickness $\tau_R(\lambda)$ and gaseous absorption optical thickness $\tau_g(\lambda)$. Within the spectral domain of the GLOBE Sun photometer the only significant gaseous absorber is ozone, so $\tau_g(\lambda)$ is approximated by $\tau_{o3}(\lambda)$. The equation for the retrieval of AOT now becomes,

$$\tau_a(\lambda) = \frac{1}{M(t)} \ln\left(\frac{\left(\frac{r_0}{r(t)}\right)^2 \cdot \left(V_{0,\lambda} - V_d\right)}{V(\lambda) - V_d} \right) - \tau_R(\lambda) - \tau_{o3}(\lambda). \quad (2.6)$$

2.4 Assumptions

In this section we investigate two assumptions that are important in calculating AOT from GLOBE LED-based Sun photometer measurements. In Eq. 2.6 it is assumed that *M(t)* is the same for τ_a, τ_R and τ_{o3}. The value of *M(t)* depends on the vertical distribution and since, in principle, aerosols, molecules and ozone have different vertical distributions, *M(t)* should be calculated separately for each component. The assumption of taking one value for *M(t)* is discussed in section 2.4.1. In Eq. 2.6 the monochromatic BBL law is applied to LEDs, that have wide spectral responses. The assumption that the monochromatic BBL law is valid for the wideband LEDs is discussed in section 2.4.2.

2.4.1 Relative air mass and vertical distribution

The relative air mass is usually interpreted as the number that quantifies the average photon path from the Sun through the atmosphere to the detector. In fact it is a number that represents the amount of scattering and absorption along the light path, relative to that for the Sun at zenith. Figure 2.2 shows the relative air mass, *M(t)* at zenith angle $\theta = \theta°$ and at zenith angle $\theta = 0°$. The light beam at zenith angle $\theta = \theta°$ in Figure 2.2 shows that the average photon path through stratospheric species, like ozone, is smaller than the average photon path through tropospheric species, like air molecules and aerosols. The light beam at $\theta = 0°$ shows that this effect does not appear at $\theta = 0°$. From this we can conclude that for large zenith angles the relative air mass in principle is different for species with different vertical distributions, while for small relative air mass this effect is negligible. Eq. 2.6 assumes that for the different components of the optical thickness the relative air masses are the same, that is,

$$e^{M_R(t)\cdot\tau_R(\lambda)} e^{M_{o3}(t)\cdot\tau_{o3}(\lambda)} e^{M_a(t)\cdot\tau_a(\lambda)} = e^{M(t)\cdot[\tau_R(\lambda)+\tau_{o3}(\lambda)+\tau_a(\lambda)]}. \quad (2.8)$$

Results from *Thomason et al* [1983] show that errors arising from different relative air masses from different vertical distributions are significant only at very large Solar zenith angles ($\theta > 70°$). Since almost all measurements are done at Solar zenith angles smaller than 70º the errors in AOT arising from wrong values for $M_{o3}(t)$ are neglected, noting that it introduces a maximum error of 0.001 AOT at large AOT and at large Solar zenith angle ($\theta > 70°$). Note that, since aerosol is assumed to peak in the troposphere, these results are applicable to measurements of tropospheric aerosol only. When large amounts of aerosol enter the stratosphere by vulcanic eruptions, errors in relative air mass may effect AOT results significantly.

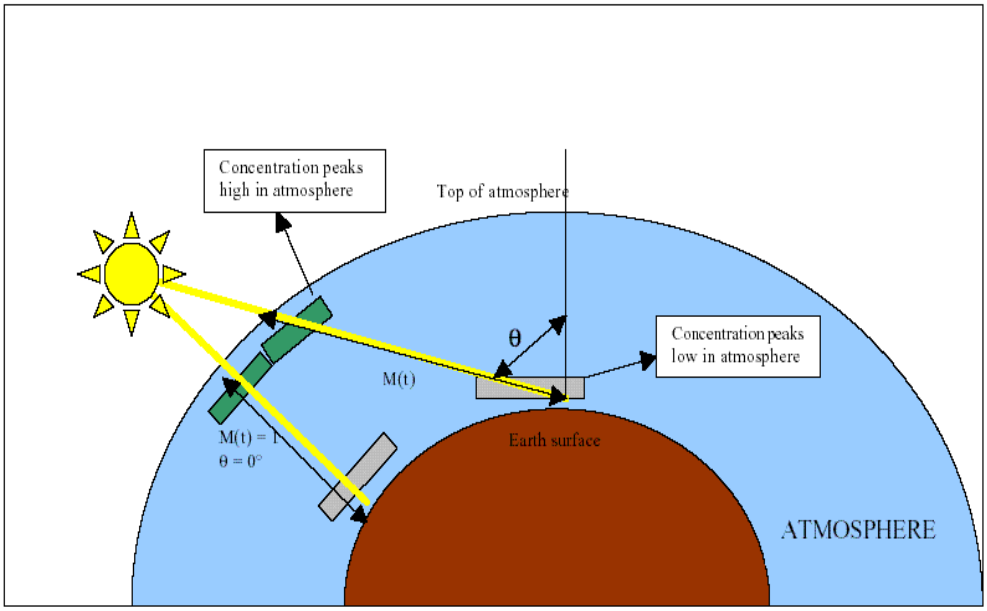

Figure 2.2. Schematic representation of the effect of vertical distribution on relative air mass. The grey bars represent air molecules and aerosols, whose concentrations peak in the troposphere. The green bars represent ozone, whose concentration peaks in the stratosphere. In practice, ozone, air molecule and aerosol concentrations have a more smooth profile.

An effect that also influences the relative air mass is refraction of the light beam in the atmosphere. The effect of refraction on relative air mass is shown in Figure 2.3. In order to determine an upper limit for errors arising from neglecting internal refraction into account, the difference in relative air mass calculations is determined at large Solar zenith angle, $\theta_{TOA} = 70.000°$ and with the atmosphere regarded as one single layer witn $n_{sealevel} = 1.00028$. Using Snellius' law of refraction, $n_1 \sin(\theta_1) = n_2 \sin(\theta_2)$, this yiels $\theta_{app} = 69.956$. This means that the errors in *M(t)* that are introduced when internal refraction is not taken into account are smaller than 0.001 and therefore this effect is not taken into account.

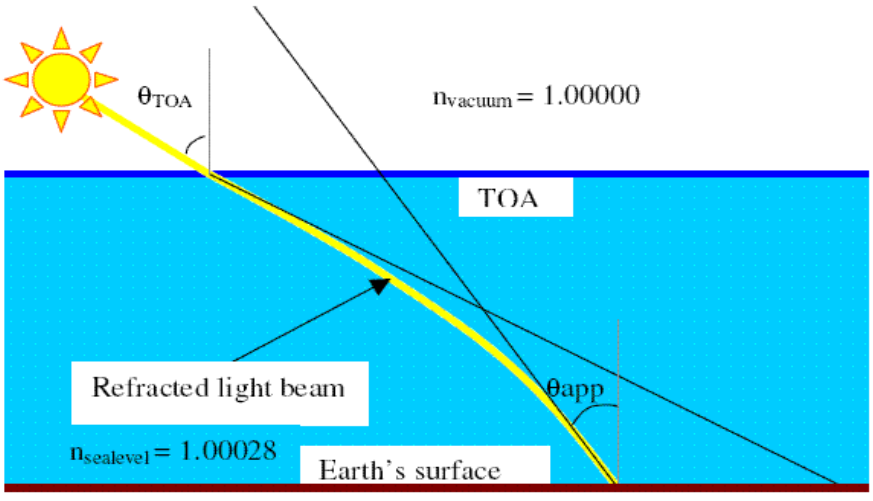

Figure 2.3. Internal refraction of a lightbeam in the atmosphere.

Now we can introduce an equation for *M(t)* without taking into account vertical distributions. The relative air mass is calculated from the Solar zenith angle θ which is a function of time, that is $\theta = \theta(t)$. The relative air mass is often approximated by sec(θ) which is called the geometric air mass, and in which the curvature of the Earth's surface and internal refraction in the atmosphere are not included. An equation for the relative air mass that takes into account the curvature of the Earth's surface and internal refraction in the atmosphere is taken from *Young* [1994],

$$M(\theta) = \frac{1.002432\cos^2\theta + 0.148386\cos\theta + 0.0096467}{\cos^3\theta + 0.149864\cos^2\theta + 0.0102963\cos\theta + 0.000303978}. \quad (2.9)$$

The difference between *M(t)* calculated using Eq. 2.9 and sec(θ) is shown in Figure 2.4. This shows that for small zenith angles sec(θ) is a very good approximation, but for $\theta > 70°$ the difference between sec(θ) an Eq. 2.9 is significant (> 0.5 %). This means that for Solar zenith angles larger then 70° the effect of a spherical Earth has a significant effect on the relative air mass and must be taken into account.

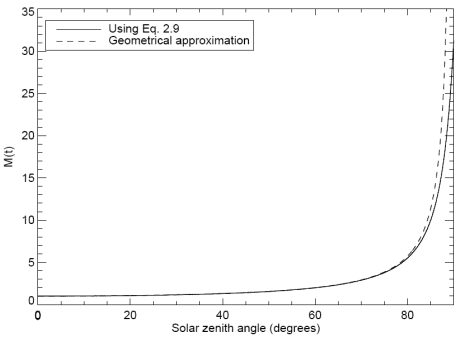

Figure 2.4. Relative air mass according to Young's formula and according to the geometrical opproximation (secθ).

2.4.2 Finite bandwith and BBL

It is all but trivial that the monochromatic BBL law can be applied to the broadband LEDs. When a detector of finite bandwith is treated as a monochromatic detector, this introduces errors that should be investigated. In professional Sun photometers, light detectors have a bandwith of typically 15 nm or less. The difference in AOT, calculated from a detector with a 15 nm bandwith with central wavelength λ_{eff} and from a monochromatic detector at λ_{eff}, is typically 0.0005 AOT. Therefore, professional Sun photometer detectors are often treated as monochromatic. The LEDs in the GLOBE Sun photometer have a bandwith of 75 nm (508 nm) and 40 nm (625 nm).

A LED measures light over a wide spectral range. In order to get AOT results at a certain wavelength, an effective wavelength for a LED is defined. Following *Brooks and Mims* [2001], the effective wavelengths for a LED with spectral response function $R(\lambda)$ is defined as,

$$\lambda_{eff} = \frac{\int_0^\infty R(\lambda) I_0(\lambda) \lambda d\lambda}{\int_0^\infty R(\lambda) I_0(\lambda) d\lambda}, \quad (2.10)$$

where $I_0(\lambda)$ is the extraterrestrial Solar irradiance at wavelength λ. The Solar irradiance at TOA, I_0, is taken rather than the radiance at the detector opening, I, in order to obtain a λ_{eff} that is independent of the conditions at the measuring site. Since the wavelength dependence of the measured radiance at the detector depends on AOT, Ångström coefficient, pressure, Ozone column and elevation of the measuring site, defining the effective wavelength at the detector (replacing I_0 in Eq. 2.10 by I) would result in a unique effective wavelength for every measurement. We note that by defining the effective wavelength we may introduce errors, whose extend is to be verified in future work.

The LED's output voltage depends on the amount of Rayleigh scattering, ozone absorption and Mie scattering by aerosols. The wavelength dependences of Rayleigh and Mie scattering cross sections, ozone absorption cross section and the response functions of the LEDs used in the GLOBE Sun photometer (HLMP-D600 and HLMP-3762) are plotted in Figure 2.5. The Rayleigh scattering cross section (solid curve) shows a λ^{-4} dependence. The Mie scattering cross section (dashed line) shows a wavelength dependence, dependent on the aerosol particle size, in the λ^{-1} - λ^{-2} range. The ozone absorption cross section (dotted curve) shows a capricious behavior. Figure 2.5 shows that the BBL law cannot simply be applied since Rayleigh, Mie and ozone cross sections have different spectrally weighted contributions at the detector. Note that the height of the curves is arbitrary and does not contain any information on the amount of scattering and absorption.

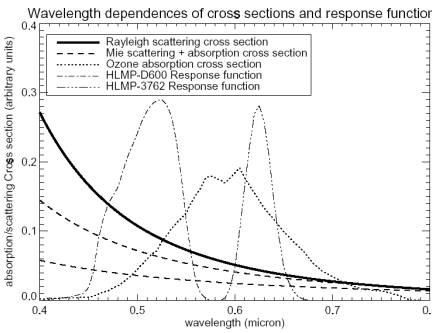

Figure 2.5. Wavelength dependence of Rayleigh scattering (λ^{-4}) (solid curve), Mie scattering and absorption (λ^{-1} and λ^{-2}) (stripes), ozone absorption (dotted curve) and the response functions of the HLMP-D600 LED (left) and the HLMP-3762 LED (right).

To account for the LED's large bandwith, the monochromatic optical thickness values that are calculated from the cross section (σ) and total column (N),

$$\tau_i(\lambda) = \sigma_i(\lambda) \cdot N_i \,, \tag{2.11a}$$

should be replaced by effective values. Effective optical thickness values $\tau_{R,eff}$ and $\tau_{o3,eff}$ for the LED's with response function $R(\lambda)$ can be defined by,

$$\tau_{i,eff} = \frac{\int_{\lambda} R(\lambda) I_0(\lambda) \tau_i(\lambda) d\lambda}{\int_{\lambda} R(\lambda) I_0(\lambda) d\lambda} \,. \tag{2.11b}$$

In general the value of $\tau_{i,eff}$ is not equal to the monochromatic value of τ_i at λ_{eff}. The effective values for Rayleigh scattering and ozone absorption at standard atmospheric conditions, that are calculated using Eq. 2.11b for the HLMP-D600 and HLMP-3762 LEDs, are listed in Table 2.1. The monochromatic Rayleigh scattering coefficients and ozone absorption coefficients for the two LEDs at the LED's effective wavelengths, that are calculated from Eq. 2.11a, are also listed in Table 2.1. Table 2.1 gives an idea of the impact of the LED's large bandwith on the Rayleigh and ozone contributions to the total optical thickness.

LED	$\tau_{R,eff}$ (eq.2.11b)	τ_R at λ_{eff} (eq.2.11a)	$\tau_{o3,eff}$ (eq.2.11b)	τ_{o3} at λ_{eff} (eq.2.11a)
HLMP-D600 (λ_{eff} = 508 nm)	0.145	0.135	0.013	0.013
HLMP-3762 (λ_{eff} = 625 nm)	0.060	0.058	0.029	0.031

Table 2.1. Rayleigh scattering and ozone absorption optical thickness at standard atmospheric conditions, effective values and monochromatic values at λ_{eff}.

The effective values for Rayleigh scattering using Eq. 2.11b and the effective values for ozone absorption using Eq. 2.11b show significant differences with the values one would obtain by taking the monochromatic optical thickness at λ_{eff}, using Eq. 2.11a. Using monochromatic optical thickness at λ_{eff} would result in systematic errors of about 0.006 AOT, and therefore the effective values, using Eq. 2.11b, are used to calculate AOT.

The transmittance of light through the atmosphere, detected by the GLOBE Sun photometer, should not be represented by the monochromatic attenuation $e^{-\tau(\lambda)\cdot M(t)}$ (Eq. 2.2), but should be represented by a transmittance function T, defined by,

$$V = V_0 * T, \tag{2.12}$$

which accounts for the full spectral range averaged by the detector. The transmittance function T is equal to the normalized spectral response of the detector,

$$T_{true} = \frac{\int R(\lambda) I_0(\lambda) e^{-M(t)\cdot[\tau_R(\lambda)+\tau_a(\lambda)+\tau_{03}(\lambda)]} d\lambda}{\int R(\lambda) I_0(\lambda) d\lambda}. \tag{2.13a}$$

Alternatively, a transmittance function using effective values can be defined, based on Eq. 2.2 and Eq. 11b,

$$T_{eff} = e^{-M(t)\cdot[\tau_{R,eff}+\tau_{o3,eff}+\tau_{a,\lambda_{eff}}]}. \tag{2.13b}$$

If these two transmittance functions give comparable results for V in Eq. 2.12, that is $T_{eff} \approx T_{true}$, then Eq. 2.13b, is a good approximation for 2.13a and $\tau_{a,\lambda eff}$ is a good measure for the aerosol optical thickness at λ_{eff}.

In order to investigate the differences in AOT results when T_{true} is approximated by T_{eff}, the behavior of the LEDs is simulated in *Brooks and Mims* [2001]. The simulation is done by calculating a Langley plot based on Eq. 2.13a with assumed aerosol optical thickness of 0.1 AOT at 508 nm. The Ångström coefficient that was used is not denoted in the article. A second Langley plot is calculated based on Eq. 2.13b (effective values). The two Langley plots are shown in Figure 2.6.

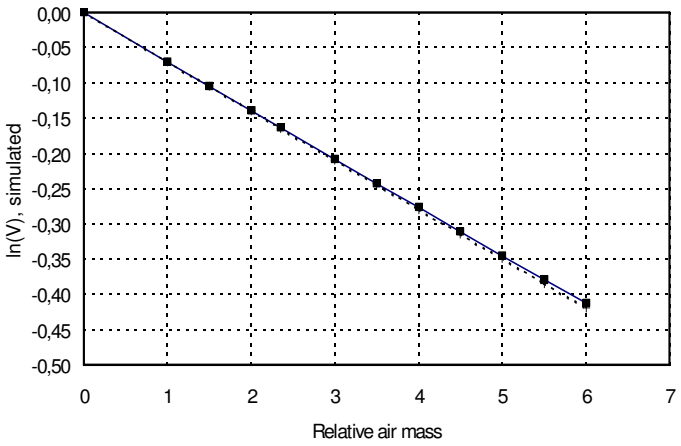

Figure 2.6. Simulated Langley plot calibrations by *Brooks and Mims* [2001] at 0.1 AOT at 508 nm. Solid line with markers: based on Eq. 2.13a. Dotted line: based on Eq. 2.13b.

At relative air masses smaller than 6 (which comes down to Solar zenith angle of 80°) the differences are negligible (< 1%), meaning that the effective value-approach can be used in that regime. This implies that the transmittance function for $M(t) < 6$ can be written as Eq. 2.13b, that is that the monochromatic BBL law can be applied to the broadband LED for relative air masses smaller then 6 and at 0.1 AOT. Since the wavelength dependence of the measured radiance at the detector depends on both AOT and Ångström coefficient, approximating Eq. 2.13a with Eq. 2.13b should also be done for a range of higher AOT values and at several values of α. This is something that should be done in future work.

2.5 Conclusion

The main conclusion of this chapter is that the monochromatic BBL law can be applied to the broadband LED-based Sun photometer. Effective values for Rayleigh scattering optical thickness and ozone absorption optical thickness should be used in AOT calculations to avoid systematic errors arising from the LED's wide spectral response. Using the geometrical air mass approximation will lead to systematic errors. Instead, the relative air mass should be calculated using Young's formula. The effect of different vertical distributions on relative air mass is negligible and therefore one single relative air mass is used for in AOT calculations. AOT measurements with the LED-based GLOBE Sun photometer are meaningful when measurements are done at relative air masses less then 6.

3 Instrument Calibration

For AOT calculation from GLOBE Sun photometer measurements the instrument's extraterrestrial constants need to be known. Since the aerosol retrieval method is sensitive to errors in the extraterrestrial constants (see chapter 4) this calibration of the instrument should be done with the highest accuracy. In order to calibrate the GLOBE Sun photometer used at KNMI (serial number: RG2-047), a Langley plot analysis is done. After calibration, RG2-047 is used as a reference instrument for relative calibration of several other instruments. The Langley plot analysis of RG2-047 is discussed in section 3.1 and the results of the relative calibrations are summarized in section 3.2. For a particular Sun photometer an accurate Langley plot calibration or a relative calibration to obtain the instrument's extraterrestrial constant $V_{0,\lambda}$ is needed only once when degradation of the LED and fluctuations of $I_0(\lambda)$ due to variations in number of Sunspots are not considered.

3.1 Langley analysis of RG2-047

A Langley plot is a plot of the instrument voltage versus relative air mass ($M(t)$). The extraterrestrial constant can be found by extrapolating a linear least squares fit to $M(t) = 0$, that is the top of the atmosphere. A Langley plot requires constant optical thickness during the measurement period and therefore stable atmospheric conditions are needed. Low AOT values are desirable, since aerosol concentrations are expected to be little variable at low AOT. Furthermore a Langley plot requires a sufficient large relative air mass range.

On several days, Langley plot measurements are done for RG2-047. The measurements performed in the morning of April 8, 2003 are used for the final calibration. This day was the best for a Langley plot analysis for the following reasons:

- 2003-04-08 was a day with relatively low AOT (0.10 at 508 nm).
- AOT was stable during the measurement time (±0.03).
- The measurements are on a straight line in the Langley plot.
- The calibration constants from these measurements give realistic AOT results ($AOT_{508nm} > AOT_{625nm}$).
- Results from the Brewer spectrofotometer at KNMI [*Allaart et al*, 2000] show a stable atmosphere with good Langley-plot conditions on 2003-04-08 (Figure 3.2).

The Langley plots from the 2003-04-08 measurements are shown in Figure 3.1.

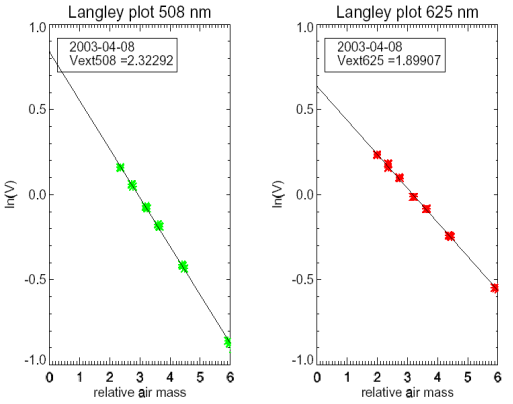

Figure 3.1. Langley plot measurements for RG2-047 taken at 2003-04-08.

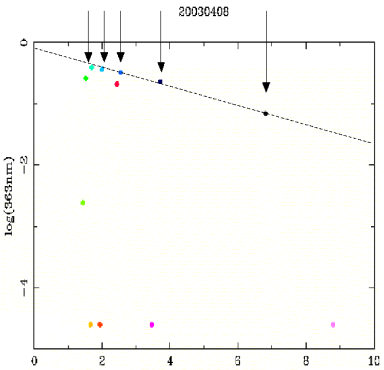

Figure 3.2. Brewer measurements (363 nm) at 2003-04-08 (Figure by M.Allaart, KNMI).

The extraterrestrial constants resulting from the linear extrapolation are 2.323 V ± 0.05 (508 nm) and 1.899 V ± 0.05 (625 nm). Figure 3.2 shows the Brewer 363 nm Langley plot at 2003-04-08. The points indicated by the arrows are measurements done in the morning, when the Langley plot measurements for RG2-047 are also done, and they lie on a relatively straight line. The other

measurements are taken in the afternoon and they show no structure because of the presence of clouds. In the morning ln(V) shows a linear dependence on $M(t)$, i.e the optical thickness is constant (at 363 nm). The uncertainty in the GLOBE $V_{0,\lambda}$'s caused by the uncertainty in the linear fit is 6 mV. However, σ_{V0} is estimated 50 mV based on results for $V_{0,\lambda}$ from other Langley plots. This uncertainty is regarded as an upper limit for the uncertainty in $V_{0,\lambda}$. The 50 mV estimation is obtained by comparing results from all Langley plots that are made for RG2-047.

3.2 Relative calibrations

All the other Sun photometers that are in use in the GLOBE Aerosol Monitoring Project in the Netherlands are calibrated relative to RG2-047. Simultaneous measurements of the instrument to be calibrated and RG2-047 are compared in order to find the response ratio, R. The simultaneous measurements are done at a range of atmospheric conditions in order to cover an as large as possible voltage range of the instrument. As an example, the resulting relative plot for RGK-204 is shown in Figure 3.3. From a linear fit to the data, R is obtained. The extraterrestrial constants are now calculated using

$$V_{0,\lambda}(instr.) = V_{0,\lambda}(RG2-047)\cdot R. \qquad (3.1)$$

The calibration constants for the Sun photometers obtained with Eq. 3.1 are listed in Table 3.1.

The precision of the $V_{0,\lambda}$'s is estimated to be 50 mV. This number comes from the uncertainty of the $V_{0,\lambda}$ of the reference instrument. The uncertainty in the fitting parameters is much smaller than 50 mV.

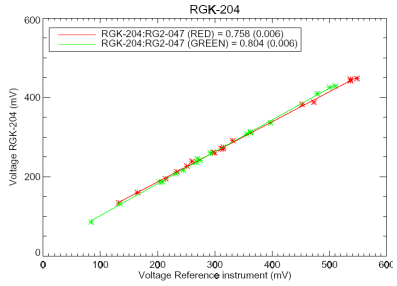

Figure 3.3. Relative calibration of RGK-204.

Serial number	$C_{instrument}$ (V) 625	$C_{instrument}$ (V) 508	user
RG2-047	1.899	2.323	KNMI
RGK-201	1.579	1.906	BN-college
RGK-202	1.443	1.440	Mozaiek
RGK-203	---------	---------	----------
RGK-204	1.440	1.867	Alkwin College
RGK-205	---------	---------	----------
RGK-206	1.385	2.361	Populier
RGK-207	1.023	1.681	----------
RGK-208	0.627	1.385	Ichthus College
RGK-209	1.332	1.848	Pascal college
RGK-210	0.956	2.048	SG. Tabor (Locatie Oscar Romero)
RGK-211	1.312	2.391	----------
RGK-212	1.289	2.027	Goois Lyceum
RGK-214	1.360	2.003	Zwin College

Table 3.1. Calibration constants and users of GLOBE Sun photometers used in the GLOBE Aerosol Monitoring project.

3.3 Conclusion

The GLOBE Sun photometer at KNMI (RG2-047) was calibrated by analysis of Langley plot measurements performed on 2003-04-08. All instruments used in the Dutch GLOBE Aerosol Monitoring Project have been calibrated relative to RG2-047. This, together with the fact that AOT results are sensitive to errors in the extraterrestrial constants, is a reason to proceed taking calibration measurements for RG2-047 to improve the precision and accuracy of the calibration.

4 Algorithm

The GLOBE program provides for an on-line algorithm that allows quick and simple processing of GLOBE Sun photometer data. In this work, an algorithm is developed independently from the GLOBE algorithm, which makes processing of data from GLOBE Sun photometer measurements possible at KNMI. The development of an algorithm at KNMI is essential for the GLOBE Aerosol Monitoring Project for the following reasons:

1. An independent algorithm makes it possible to compare the algorithm with the GLOBE algorithm, which may lead to improvements.
2. The development of an algorithm improves the error analysis, and thus improves the quantitative estimate of the uncertainty associated with AOT results at KNMI.
3. The development of an algorithm gives insight into the sensitivities of AOT calculation.

The equation governing the AOT calculation from the instrument's voltage is presented in section 4.1 and is tested by comparing results with results from the on-line GLOBE algorithm. The KNMI – GLOBE algorithm comparison is presented in section 4.2. The error analysis is discussed in section 4.3 and the conclusions are presented in section 4.4.

4.1 AOT Calculation

Following Eq. 2.6 with the effective values for the Rayleigh and ozone coefficients from Table 2.1 and subtracting the instrument's dark voltage V_d (that is the voltage obtained from the instrument in total darkness) from V and V_0,, we obtain the equation used in the algorithm to retrieve AOT from GLOBE Sun photometer measurements,

$$\tau_a(\lambda_{eff}) = \frac{1}{M(t)} \cdot \ln\left(\frac{\left(\frac{r_0}{r(t)}\right)^2 \cdot (V_{0,\lambda} - V_d)}{V_{\lambda_{eff}} - V_d} \right) - \tau_{R,eff}(p) - \tau_{o3,eff}(N), \tag{4.1}$$

where N denotes the overhead ozone column in Dobson Units (DU), p denotes the pressure and we write $M(t)$ explicitly to illustrate the that the relative air mass is a function of measurement time. We will discuss all the elements in the equation:

- $M(t)$ is the relative air mass which depends on the time of measurement. $M(t)$ is calculated from the Solar zenith angle, θ, using Eq. 2.9. The Solar zenith angle is calculated using $\cos(\theta) = \sin(\varphi)\sin(\delta)+\cos(\varphi)\cos(\delta)\cos(h)$ where φ is the latitude, δ the declination of the Sun and h is the hour angle. The declination of the Sun is calculated using the equation given by *Liou* [2002]. Measurements with $M(t) > 6$ are rejected because systematic errors become significant at $M(t) > 6$ (see section 2.4.2).
- $(r_0/r)^2$ accounts for the fluctuations in TOA irradiation due to the non-spherical orbit of the Earth around the Sun. Its value depends on the measurement time and has a one-year period in which it ranges between 1.034 on January 3 and 0.967 on July 5 [*Liou,* 2002].
- $V_{0,\lambda}$ is the extraterrestrial constant of the instrument's channel. It is determined by a Langley plot analysis that is discussed in section 3.1. The extraterrestrial constant is determined for an Earth-Sun distance of 1 AU, so $V_{0,\lambda}$ is interpreted as the voltage the instrument would measure at TOA at 1 AU. The value of $V_{0,\lambda}$ depends on the components of the instrument. $V_{0,508}$ is in general not equal to $V_{0,625}$. For most Sun photometers the values of the extraterrestrial constants range between 1000 mV and 2200 mV.
- V_d is the dark voltage, that is the instrument voltage in total darkness. It is measured by sealing off the detector opening and denoting the output voltage. It is always less than 20 mV.
- $V_{\lambda eff}$ is the instrument voltage, the actual measurement. It is obtained by pointing the Sun photometer opening at the Sun, aligning it, and denoting the maximum output voltage in a period of 10 seconds for a cloud-free Soalr disk. Its value depends on the relative air mass and the total optical thickness of the atmosphere. Its value is somewhere between V_d and V_0, except for values close to V_0 because there is always a certain amount of Rayleigh scattering and ozone absorption present in the lightpath.

- The Rayleigh scattering effective optical thickness, $\tau_{R,eff}(p)$, is calculated from the effective coefficients in Table 2.1 and the surface pressure, $\tau_{R,eff}(p) = p/p_0 \cdot \tau_{R,eff}$. The standard pressure, p_0, is taken 1013 mbar. The pressure is obtained by KNMI meteo data for measurements done at KNMI, and by a barometer for GLOBE students. At sea level, the pressure normally ranges between 980 and 1040 mbar in the Netherlands, which makes the effective Rayleigh coefficients about 0.14 (508 nm) and 0.06 (625 nm). Since AOT generally ranges between 0.05 and 0.5 Rayleigh scattering is a relatively large component of the optical thickness at 508 and 625 nm.
- The ozone absorption effective optical thickness, $\tau_{o3,eff}(N)$, is calculated from the effective coefficients in Table 2.1 and the ozone column, $\tau_{o_3,eff}(N) = N/N_0 \cdot \tau_{o_3,eff}$ The standard ozone column, N_0, is taken 300 DU. The total ozone column is obtained by Brewer UV ozone measurements for measurements done at KNMI [*Allaart et al*, 2000]. For measurements done by GLOBE students the ozone column is determined at KNMI by extrapolating Brewer UV ozone measurements to the GLOBE school measuring location. Since the ozone column over the Netherlands can have significant gradients this extrapolating introduces errors that should be accounted for in the error analysis. However, the ozone column gradient is usually small at clear and stable atmospheric conditions at high atmospheric pressure, when most GLOBE AOT measurements are done. Normally the ozone column ranges between 250-400 DU which makes the effective ozone absorption coefficients range between 0.01 and 0.02 (508 nm) and between 0.02 and 0.04 (625 nm). Ozone absorption contributes less to the optical thickness than Rayleigh scattering, but the ozone absorption contribution is a significant component and should therefore be included.
- The metadata is written down directly after the measurement. This is the data that describes the conditions during the measurement and contains information on temperature, cloud cover, cloud types, sky color, haziness and all other reasons for obscured sky. Accurately registering metadata provides additional value to the GLOBE AOT measurements that AOT measurements done with a fully automatic instrument usually lack. The check with metadata can be used to expel measurements performed under bad conditions and is therefore an essential feedback system in the measurement method of the GLOBE Sun photometer.

The algorithm that is developed in this work is shown in a flowchart in Figure 4.1. The check with the metadata is essential in the decision to accept or reject data and is represented by the dashed line. If the data is rejected, then it is not stored.

Eq. 4.1 assumes that the only significant absorber within these two wavelength ranges is ozone. H_2O also absorbs in this wavelength regime. The H_2O absorption cross-section has order of magnitude $1 \cdot 10^{-26}$ molecules$\cdot$cm^{-2} for both channels. Over the Netherlands the water vapor column ranges between 0 - 35 kg$\cdot$m^{-2} [*De Haan and Barlag*, 2003]. This gives a maximum contribution of H_2O to the optical thickness of $1 \cdot 10^{-3}$ for measurements done in the Netherlands. This is very small compared to Rayleigh scattering and ozone absorption and therefore it is not included in the algorithm.

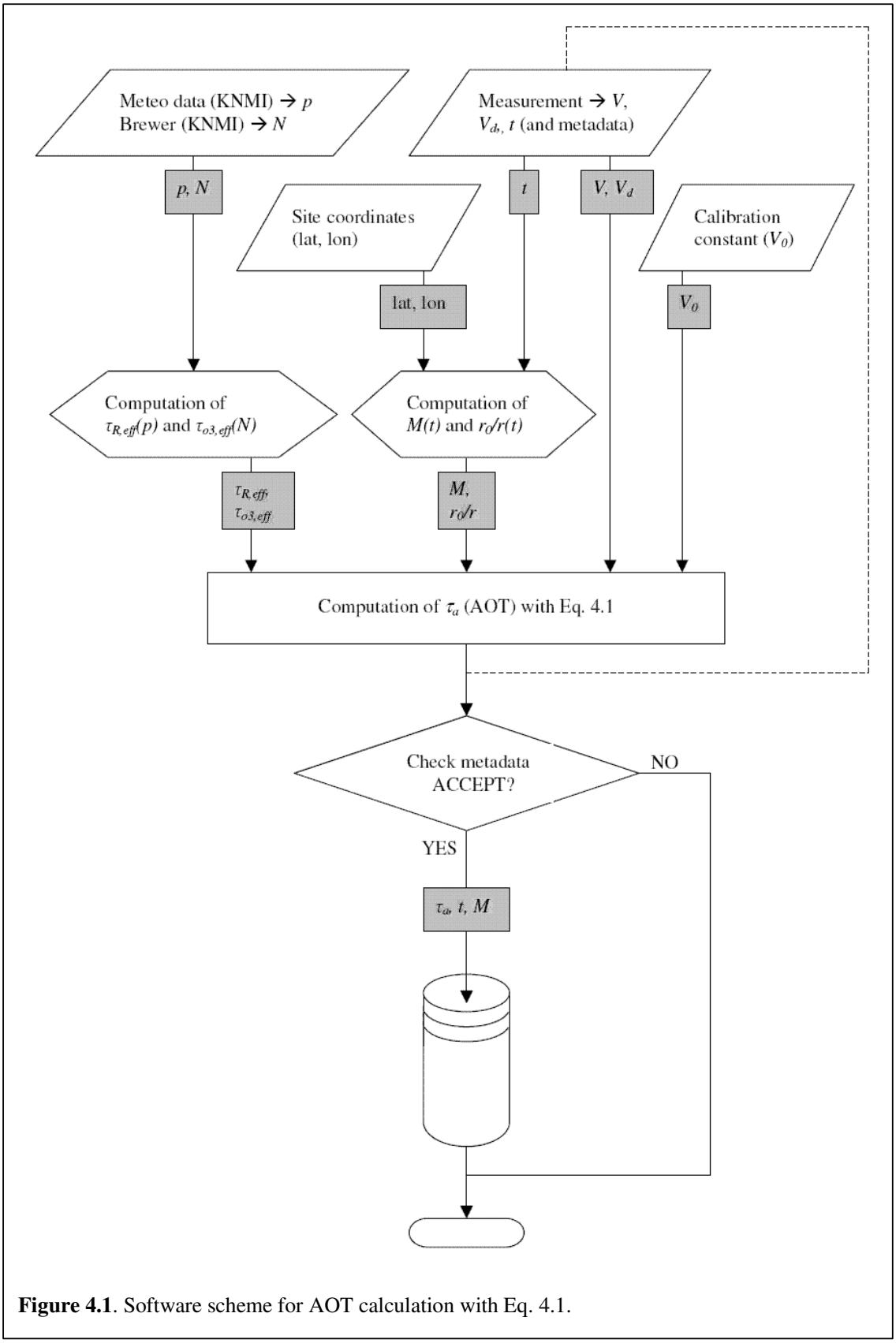

Figure 4.1. Software scheme for AOT calculation with Eq. 4.1.

The results of GLOBE Sun photometer measurements at De Bilt are shown in Figure 4.2. The measurements are done in the framework of this thesis and are done on the roof of KNMI in the period September 2002– August 2003 with Sun photometer RG2-047. The AOT measurements have the expected range (0.0 - 0.4) for De Bilt [*Stammes and Henzing,* 2000]. Furthermore, AOT values at 508 nm are higher than AOT values at 625 nm, consistent with Ångström's relation (Eq. 2.1).

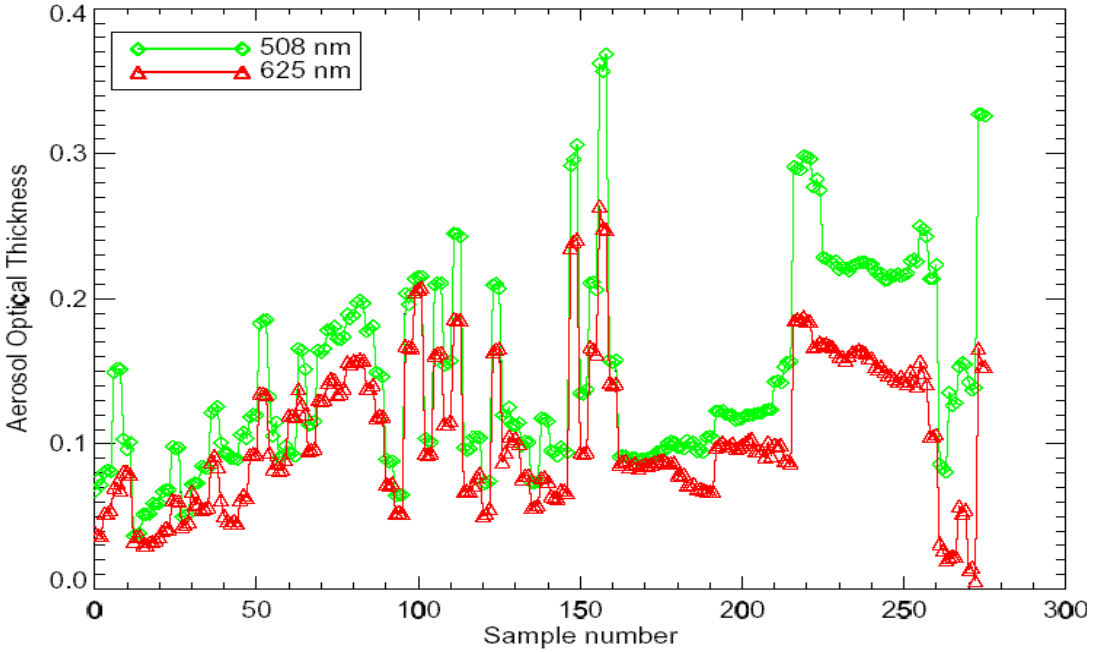

Figure 4.2. AOT time series for GLOBE Sun photometer measurements at De Bilt in the period 2002-09 – 2003-08

4.2 Algorithm comparison

In order to check the KNMI algorithm, measurements done at KNMI in the period September 2002 – April 2003 processed by both the KNMI and the GLOBE algorithm are compared. The mean difference between the KNMI algorithm and the GLOBE algorithm is shown in Table 4.1. Most of the difference between the KNMI and GLOBE algorithm is be caused by ozone correction in the KNMI algorithm. The GLOBE algorithm does not correct for ozone absorption [*Brooks, private comm.* 2003]. The agreement between KNMI and GLOBE algorithms when ozone absorption is not included in the KNMI algorithm improves greatly, as is shown in Table 4.1 by the mean difference Δ.

Algorithms	Δ 508 nm (AOT)	Δ 625 nm (AOT)
KNMI - GLOBE	-0.024	-0.039
KNMI(no ozone) - GLOBE	-0.003	-0.004

Table 4.1. Difference of AOT results from KNMI and GLOBE algorithms with and without ozone absorption included in the KNMI algorithm.

From the results in Table 4.1 it is clear that the main cause of the difference in AOT between the two algorithms is ozone absorption. The calculations in section 4.2 have shown that ozone is a significant contributor to the optical thickness. Not accounting for ozone absorption will lead to an overestimation of AOT. When ozone absorption is not taken into account in the KNMI algorithm the mean difference is reduced one order of magnitude. The difference while leaving ozone out of the KNMI algorithm is plotted as a function of relative air mass for both the 508 and 625 nm channels in Figure 4.3.a. In

Figure 4.3.b, the difference is plot as a function of $M(t)^{-1}$, which shows a linear relation suggesting that the resulting difference is caused by differences in relative air mass calculations. Therefore the computation of relative air mass in both the KNMI and GLOBE algorithm is investigated. The difference in relative air mass between KNMI and GLOBE is plot as a function of relative air mass in Figure 4.4. The difference in relative air mass is very small (0.1 %) and the difference in AOT cannot be explained by the difference in relative air mass alone. The Rayleigh effective optical thickness used by the GLOBE algorithm has also shown to differ slightly from the values presented in Table 2.1, and this also accounts for part of the difference between KNMI and GLOBE results.

When ozone is left out of the KNMI algorithm the two algorithms compare up to 0.006 AOT which is a very good agreement. Small differences between Rayleigh coefficients and between relative air mass calculations account for very small AOT differences between the two algorithms.

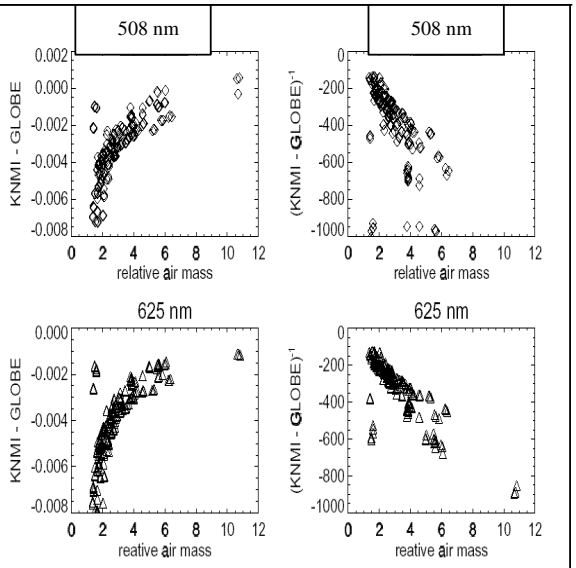

Figure 4.3. $M(t)^{-1}$ dependence of AOT differences between KNMI (no ozone) and GLOBE algorithms.

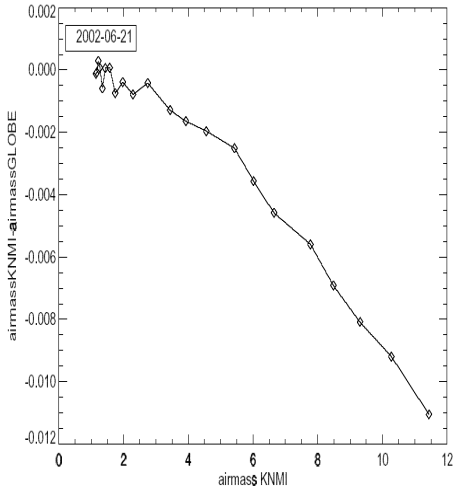

Figure 4.4. Difference in relative air mass between KNMI and GLOBE algorithms (calculations done for June 21, 2002)

4.3 Error analysis

A quantitative error analysis is essential for the GLOBE Aerosol Monitoring Project. The validation of satellite measurements with GLOBE Sun photometer AOT measurements requires accuracy and precision esimates of GLOBE Sun photometer AOT measurements. Furthermore a qualitative error analysis gives information about the conditions at wich GLOBE Sun photometer measurements are most reliable.

4.3.1 Random Errors

The uncertainty in AOT, $\Delta\tau_a$, is determined by the uncertainties in the individual parameters in Eq. 4.1. Since $\tau_a = f(r/r_0, V_0, V, t, lat/lon, p, N)$, we need to know the uncertainties Δx_i of parameters x_i and how they propagate in Eq. 4.1, in order to compute $\Delta\tau_a$.

A measure for the uncertainty in the measurement of τ_a is the standard deviation $\sigma_{\tau a}$. Since uncertainties in V_0, V, t, p and N are independent, the equation that relates the standard deviation and the variance to the uncertainty in each of the individual parameters is,

$$\sigma_{\tau_a}^{\ 2} = \left\langle \varepsilon_{\tau_a}^{\ 2} \right\rangle = \sum_i \left(\frac{\partial \tau_a}{\partial x_i} \sigma_{x_i} \right)^2 , \qquad (4.3)$$

where $\partial\tau_a/\partial x_i$ is the sensitivity of τ_a to parameter x_i, that is obtained by differentiating Eq. 4.1 with respect to parameter x_i. We will now discuss the contribution of all the parameters to $\sigma_{\tau a}$, which comes down to finding $(\partial\tau_a/\partial x_i)\sigma_{xi}$ for every x_i.

Due to very low sensitivity of τ_a to uncertainties in site coordinates, combined with precisely known locations, the *lat/lon* uncertainties are neglected in the analysis. The same argumentation holds for r_0/r.

4.3.1.1 Sensitivity to extraterrestrial constant uncertainties

The uncertainty in V_0, σ_{V0}, is estimated to be 50 mV in section 3 and applies to all Sun photometers. This is an upper limit that arises from the uncertainty in the linear regression of the Langley plot, the spread in the results of the other Langley plots and the uncertainty in the response ratio for the relative calibrated instruments. The sensitivity of τ_a to V_0 is given by differentiating Eq. 4.1 with respect to V_0,

$$\frac{\partial \tau_a}{\partial V_{0,\lambda}} = \frac{1}{M(t)(V_{0,\lambda} - V_d)} . \qquad \text{(Eq. 4.4)}$$

Figure 4.5.a shows the sensitivity of AOT retrieval to $V_{0,\lambda}$. The figure is obtained for typical values of the other parameters: V = 700 mV, $M(t)$ = 2, $p = p_0$, $N = N_0$ for a range of $V_{0,\lambda}$.

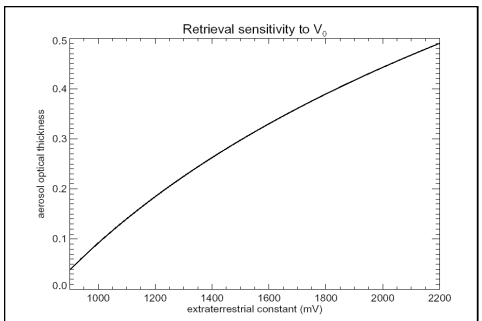

Figure 4.5.a. Sensitivity to extraterrestrial constant.

The slope in Figure 4.5.a represents the sensitivity of the retrieval to uncertainties in V_0 and is equal to the analytical expression given above. The figure shows a $V_{0,\lambda}^{-1}$ dependence and from the analytical expression we note that there is also an $M(t)^{-1}$ dependence. From this we conclude that the retrieval of τ_a is more sensitive to the uncertainty in $V_{0,\lambda}$ for instruments with small $V_{0,\lambda}$ and for measurements at small relative air mass.

4.3.1.2 Sensitivity to voltage uncertainties

The uncertainty in V, σ_V, is estimated at 5 mV for measurements done at KNMI. This number arises from alignment errors and the large response time of the voltmeter (≈ 1 second). For measurements done by GLOBE school students, who are less experienced, σ_V for individual measurements ranges from 5 mV up to sometimes 70 mV. For every individual measurement, σ_V should be examined, but this implies unrealistic off-line inspection of measurement forms. Instead, every school is assigned a standard σ_V based on voltage ranges from previous measurements. A GLOBE AOT measurement consists of three Solar radiance measurements done closely after each other and the mean spread of the voltages from these three measurements is taken as the standard σ_V. The sensitivity of τ_a to V is given by differentiating Eq. 4.1 with respect to V,

$$\frac{\partial \tau_a}{\partial V} = \frac{-1}{M(t)(V - V_d)} . \qquad \text{(Eq. 4.5)}$$

Figure 4.5.b shows the sensitivity of AOT retrieval to V with V_0 = 2200 mV, $M(t)$ = 2, $p = p_0$, $N = N_0$.

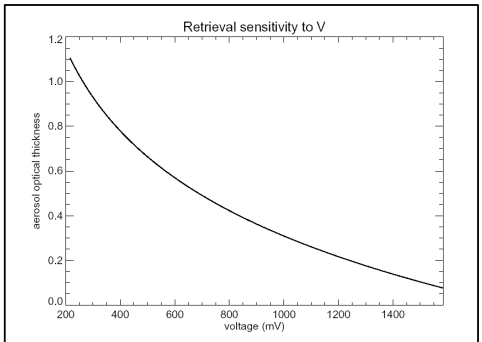

Figure 4.5.b. Sensitivity to Voltage.

The slope in Figure 4.5.b shows a $-V^{-1}$ dependence and from the analytical expression we note that there is an $M(t)^{-1}$ dependence. From this we conclude that

the retrieval of τ_a is more sensitive to the uncertainty in voltage for small voltages and for measurements at small relative air mass.

4.3.1.3 Sensitivity to time uncertainties

The uncertainty in *t*, σ_t, is estimated at 60 seconds for measurements done at KNMI as well as for GLOBE student measurements. This arises from deviations of the measurement clock from UT and from the fact that some students report the measurement time in minutes instead of seconds. The sensitivity of τ_a to *t* is given by differentiating Eq. 4.1 with respect to *t*,

$$\frac{\partial \tau_a}{\partial t} = \frac{\partial \tau_a}{\partial M(t)} \frac{\partial M(t)}{\partial t} = \frac{-1}{M(t)^2} \ln\left(\frac{\frac{r}{r_0} * \left(V_{0,\lambda_{eff}} - V_d\right)}{V_{\lambda_{eff}} - V_d} \right) \frac{dM(t)}{dt}, \qquad \text{(Eq. 4.6)}$$

in which *dM(t)/dt* is computed numerically.
Figure 4.5.c shows the sensitivity of AOT retrieval to *t* for, $M(t) < 6$, for June 21, December 21, and September 21, with $V_0 = 2200$ mV, $V = 700$ mV, $p = p_0$, $N = N_0$.

Figure 4.5.c shows that the retrieval of τ_a is very sensitive to the uncertainty in *t* at Sunrise and Sunset, and that it is more sensitive in summer than in winter.

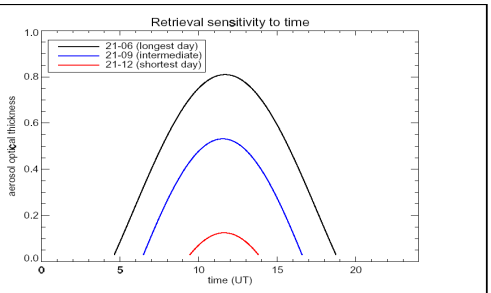

Figure 4.5.c. Sensitivity to time (M(t)< 6).

4.3.1.4 Sensitivity to pressure uncertainties

The uncertainty in pressure, σ_p, is estimated at 1 mbar for measurements done at KNMI. This number is estimated from the precision of KNMI meteo data. For GLOBE school students, σ_p is estimated 5 mbar. This is determined from the precision at which a simple barometer is expected to measure pressure. The sensitivity of τ_a to *p* is given by differentiating Eq. 4.1 with respect to *p*,

$$\frac{\partial \tau_a}{\partial p} = \frac{-\tau_{R,eff}}{p_0}. \qquad \text{(Eq. 4.7)}$$

Figure 4.5.d shows the sensitivity of AOT retrieval to *p* with $V_0 = 2200$ mV, $V = 700$ mV, $M(t) = 2$, $N = N_0$.

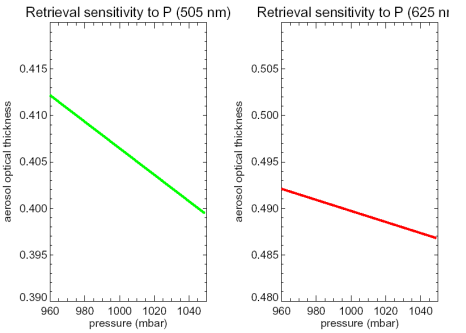

Figure 4.5.d. Sensitivity to pressure.

From Figure 4.5.d and the analytical expression it is clear that the sensitivity of the retrieval of τ_a to pressure does not depend on pressure and is therefore constant. Figure 4.5.d shows furthermore that the green channel is somewhat more sensitive to pressure uncertainties that the red channel, which is consistent with the larger Rayleigh optical thickness for the green channel.

4.3.1.5 Sensitivity to ozone column uncertainties

The uncertainty in ozone column, σ_N, is estimated at 5 DU for measurements at KNMI. This number arises from the precision of the Brewer ozone column measurements. For GLOBE student measurements, σ_N is estimated 15 DU. This number is estimated from the precision of Brewer ozone column measurements combined with typical values of the gradient of the ozone column over the Netherlands. The sensitivity of τ_a to *N* is given by differentiating Eq. 4.1 with respect to *N*,

$$\frac{\partial \tau_a}{\partial N} = \frac{-\tau_{o_3,eff}}{N_0}. \qquad \text{(Eq. 4.8)}$$

Figure 4.5.e shows the sensitivity of AOT retrieval to N with V_0 = 2200 mV, V = 700 mV, $M(t)$ = 2, p = p_0.

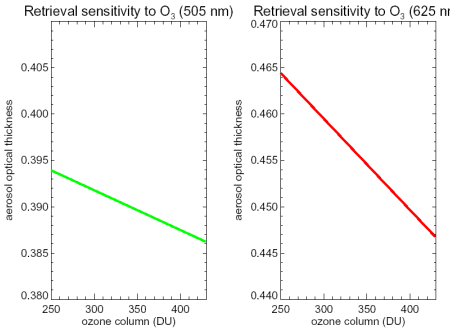

Figure 4.5.e. Sensitivity to ozone column.

From Figure 4.5.e and the analytical expression it is clear that the sensitivity of the retrieval of τ_a to the ozone column is constant. Figure 4.5.e shows furthermore that the red channel is somewhat more sensitive to the ozone column uncertainty than the green channel, which is consistent with the larger ozone optical thickness for the red channel.

4.3.1.6 Total uncertainty in τ_a

We can now calculate the total uncertainty in τ_a by squaring and adding the partial uncertainties of the individual parameters according to Eq. 4.3. In order to find out which parameters contribute significantly to the total uncertainty, the mean partial uncertainties for 508 and 625 nm measurements at KNMI in the period September 2002 – April 2003 (as plotted in Figure 4.2) are listed in Table 4.2. The total mean uncertainty in τ_a is given in the bottom row. The results show that the main contributor is $V_{0,\lambda}$. This is due to the large uncertainty in $V_{0,\lambda}$. The contributions from V and t are comparable, but both smaller than the $V_{0,\lambda}$ contribution. The contributions from p and N are both negligibly small.

x_i	Mean 508 nm	Mean 625 nm
σ_{V0}	0.009	0.01
σ_V	0.002	0.002
σ_t	0.001	0.001
σ_p	0.0001	0.0001
σ_N	0.0002	0.0005
==	=====	=====
$\sigma_{\tau a}$	0.01	0.01

Table 4.2. Partial uncertainties. Results from KNMI measurements in the period September 2002 – April 2003.

Figure 4.6 shows the partial uncertainties of all measurements in the September 2002 – June 2003 period as a function of measurement time in UT. The total uncertainty in AOT as a function of UT is plotted at the bottom of Figure 4.6.The uncertainty in AOT is always less than 0.02 AOT. Figure 4.6 shows that $\sigma_{\tau a}$ is dominated by $\sigma_{V0,\lambda}$, and that the uncertainty is high for measurements done in the middle of the day, due to the $M(t)^{-1}$ dependence of the $V_{0,\lambda}$ sensitivity. For measurements done at high Solar zenith angles (and consequently high $M(t)$) there is a significant influence of σ_t. In the middle of the day, the contribution of σ_v exceeds the contribution of σ_t, but they are both much smaller there than $\sigma_{V0,\lambda}$. These results show that it is essential that $V_{0,\lambda}$ is determined with higher precision. When $V_{0,\lambda}$ is determined more accurately, the precision of GLOBE AOT measurements can get up to 0.01 AOT.

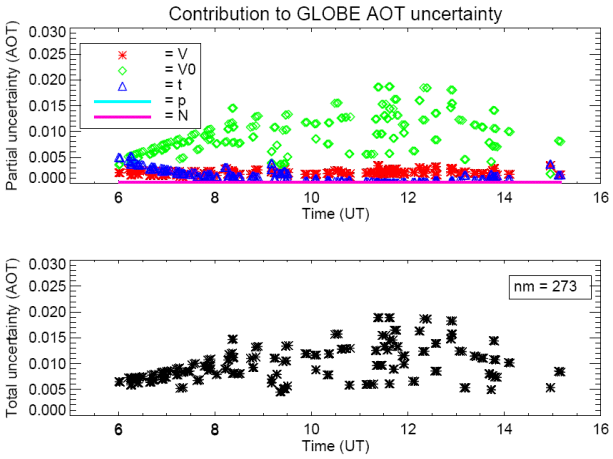

Figure 4.6. Time dependence of partial uncertainties for all measurements in the period September 2002 – June 2003

4.3.2 Systematic errors

Systematic errors in the AOT values may occur due to wrong values for instrumental constants, or unknown correlations between algorithm parameters. In order to check for unknown correlations the correlation coefficients of AOT with several parameters are calculated for the KNMI dataset and the Populier dataset. The results are listed in Table 4.3. Pressure and temperature correlation coefficients are all very small which indicates that there is no correlation between AOT and pressure and temperature. There is a weak correlation between ozone column and GLOBE AOT from KNMI, but AOT from The Hague shows no correlation with ozone column. Wrong values for V_0 will also lead to systematic errors. We try to account for that by a large estimate of the uncertainty of V_0, but it may still be a source of systematic errors.

Parameter	r (KNMI)	r (Populier)
Pressure	0.06	0.05
Temperature	0.06	0.39
Ozone column	0.63	-0.17

Table 4.3. Correlation coefficients with AOT (508 nm)

Sub-visible cirrus clouds lead to systematically too high AOT values. There are cirrus measurements done by satellites in the IR, but this only gives information on cirrus clouds during the satellite overpass time. Therefore we cannot determine the extend of errors due to cirrus clouds. Systematic errors may be found by comparison between GLOBE Sun photometer measurement and measurements from a professional Sun photometer. This is discussed in the next chapter.

4.4 Conclusion

The development of an aerosol optical thickness algorithm at KNMI has been very useful for the GLOBE Aerosol Monitoring Project at KNMI. GLOBE Sun photometer AOT results computed with the algorithm show agreement to within 0.006 AOT with the GLOBE values The most important difference with the GLOBE algorithm is the inclusion of ozone absorption in the KNMI algorithm. Not including ozone absorption will lead to an overestimation of 0.01 - 0.04 AOT. Different calculations of the relative air mass and differences in Rayleigh scattering coefficients give rise to very small, negligible differences between the KNMI and GLOBE algorithm. The uncertainty in AOT from the theoretical error analysis is smaller than 0.02 for both channels. The main contribution to this uncertainty comes from the extraterrestrial constants. Since the algorithm is very sensitive to errors in $V_{0,\lambda}$ in the middle of the day, measurements done in the morning and evening have the best precision. However, when $V_{0,\lambda}$ will be known more accurately in future, parameters such as V and t, with other sensitivity profiles may contribute significantly to the total uncertainty in AOT.

5 Validation of GLOBE AOT measurements

In *Brooks and Mims* [2001], GLOBE AOT measurements are compared to AERONET AOT measurements and agreed up to a few percent. Where in the previous section the theoretical error analysis was discussed, is the purpose of this section to investigate the accuracy and precision of Dutch GLOBE AOT measurements in practice. Therefore a quantitative estimate of the accuracy and precision of GLOBE AOT measurements is necessary. Comparisons of GLOBE Sun photometer AOT measurements with AOT measurements from a professional Sun photometer at KNMI are used to investigate how accurately and precise GLOBE students theoretically should be able to measure AOT with the GLOBE Sun photometer. This is discussed in section 5.1. GLOBE AOT measurements done at "Christelijk College De Populier" in The Hague are used to investigate how accurately and precisely GLOBE students measure AOT in practice. This is discussed in section 5.2. The reason to use measurements from the The Hague school, which is therefore a key-school in the project, is that there is a professional Sun photometer at TNO-FEL in The Hague so that results from GLOBE and TNO-FEL can be compared. The results from the comparison are used to estimate the accuracy and precision at which students from ''De Populier'' measure AOT in practice. The conclusions are presented in section 5.3. The results of this section are essential to the project since it establishes a practical accuracy and precision of Dutch GLOBE AOT measurements and consequently shows if satellite instrument validation by Dutch GLOBE AOT measurements is useful.

5.1 Validation of GLOBE Sun photometer AOT measurements with SPUV AOT measurements.

In order to check the quality of GLOBE AOT measurements, measurements taken at KNMI from September 2002 - March 2003 are compared to AOT measurements from the Sun Photometer Ultra Violet (SPUV) at KNMI. The GLOBE AOT measurements are done on the roof of KNMI, next to the SPUV. The SPUV is an extensively calibrated, professional Sun photometer. The SPUV is placed on a Sun tracker that enables automatic Solar radiance measurements during the whole day. The SPUV measures Solar radiance at 368 nm, 501 nm, 674 nm, 780 nm, 870 nm and 940 nm with a bandwith of about 15 nm and with a sampling time of 60 seconds. For a detailed description of the measuring method of the SPUV, see *Hasekamp* [1998]. The 940 nm channel is not used for the comparison, since strong water vapor absorption makes AOT retrieval for this channel troublesome. Normally, AOT from SPUV measurements is calculated using a Langley plot analysis, which results in an AOT averaged over the measurement time which is a few hours. Since GLOBE measurements are instantaneous, comparing with SPUV time averaged AOT is not desirable. Therefore, AOT is calculated from SPUV measurements by processing direct SPUV output using the algorithm for the GLOBE Sun photometer. This has the additional advantage of preventing AOT differences arising from algorithm differences.

SPUV AOT values should be interpolated to the GLOBE wavelengths, that is to 508 nm and 625 nm, in order to make a useful comparison. The SPUV measurements fit the Ångström relation well, except for the measurements at 674 nm. This makes exponential interpolation following the Ångström relation questionable. To illustrate the difference between exponential interpolation using SPUV 501 nm and 780 nm and linear interpolation using 501 nm and 674 nm the mean SPUV AOT results from 1997 – 2002 are plotted in Figure 5.1. The exponential curve is obtained by fitting a $\lambda^{-\alpha}$ curve to the SPUV data points with omission of the 674 nm channel, where α is the mean Ångström coefficient, which is 1.398. The dashed line is a linear fit between the 501 and 674 nm SPUV AOT values. Figure 5.1 shows that the AOT values at 508 nm, obtained by linear and exponential interpolation, are within 0.0005 AOT, suggesting that the interpolated SPUV AOT at 508 nm is not sensitive to the interpolation method. The AOT value at 625 nm obtained by linear interpolation is about 0.02 higher than the value obtained by exponential interpolation suggesting that the interpolated 625 nm SPUV AOT is sensitive to the interpolation method and different interpolation methods may lead to AOT differences as large as 0.02 AOT.

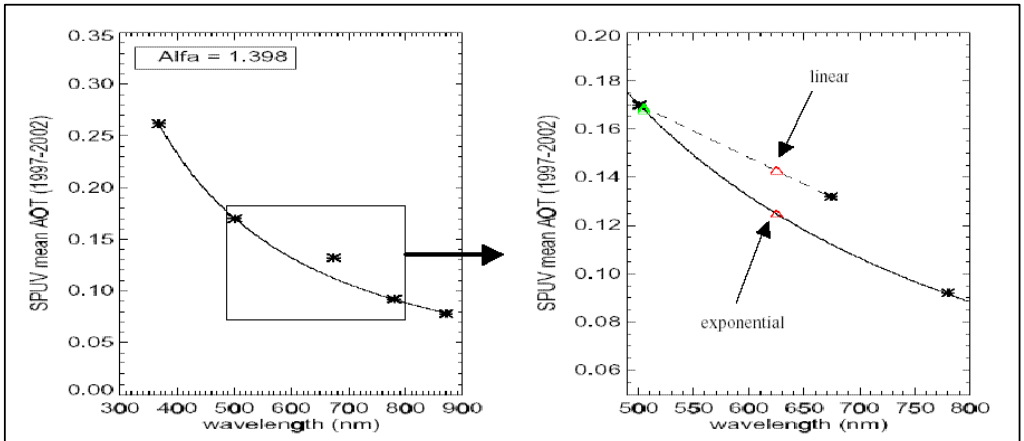

Figure 5.1. Difference between linear and exponential interpolation of SPUV AOT data between 501 nm and 674 nm.

A third interpolation method, which is not shown in Figure 5.1, is exponential interpolation between 501 and 674 nm. 138 measurements, from September 2002 – March 2003, from GLOBE KNMI and SPUV are compared using the three interpolation methods. In Table 5.1 the correlation coefficients for GLOBE and SPUV AOT and the mean differences, Δ, (GLOBE - SPUV) are shown for the three interpolation methods. As expected, 508 nm results are not sensitive to the interpolation method. For 625 nm the results are best with the exponential interpolation method using 501 nm and 780 nm. From these results, and the fact that the exponential methods using 780 nm is in better agreement with the Ångström relation, this method is used for the analysis, thereby rejecting SPUV 674 nm AOT value.

	r (508 nm)	r (625 nm)	Δ (508 nm)	Δ (625 nm)
Linear	0.97	0.93	-0.013	-0.021
Exp. (501 & 674)	0.97	0.93	-0.013	-0.020
Exp. (501 & 780)	0.97	0.96	-0.006	-0.007

Table 5.1. Correlation coefficients and mean differences of the three interpolation methods.

The scatter plots for GLOBE and SPUV coincident measurements, for 508 nm and 625 nm, using exponential interpolation method with the 501 nm and 780 nm channels are shown in Figure 5.2. The correlation coefficients are 0.97 (508 nm) and 0.96 (625 nm). The 508 nm channel shows some points, at 0.2 AOT, where GLOBE does not match SPUV. This may be due to clouds, although there was no report of any clouds for the GLOBE measurements. The scatter is largest for the 625 nm channel. In order to find the cause of the scatter and deviation from the $y = x$ line, the GLOBE Sun photometer 508 nm output (voltage) and the SPUV 501 nm output (counts) are directly compared, after correction for the dark voltage. The resulting scatter plot is shown in Figure 5.3, the

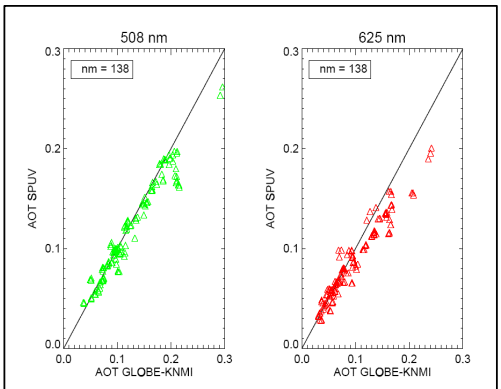

Figure 5.2. Correlation between GLOBE AOT and SPUV AOT at 505 nm and 625 nm.

correlation coefficient is 0.9997, which is practically one. The extreme good correlation suggests that the scatter and the deviation from the $y = x$ line in Figure 5.2 may be improved by recalibration of the extraterrestrial constants, from either the SPUV or GLOBE Sun photometer, or both. If the scatter and deviation from $y = x$ is due to errors in $V_{0,\lambda}$, a correlation between the AOT difference and $M(t)^{-1}$ is expected based on Eq. 4.4. Figure 5.4 shows the difference between GLOBE and SPUV AOT as a function of $M(t)^{-1}$. There is a weak negative correlation for both channels. This indicates that either the GLOBE extraterrestrial constants or the SPUV extraterrestrial constants are not accurately enough determined. From the Figures 5.2 till 5.4 we conclude that the GLOBE Sun photometer voltage measurements can in principle be used for AOT retrieval. However, the extraterrestrial constants should be known more accurately in order to achieve a better correlation with professional measurements.

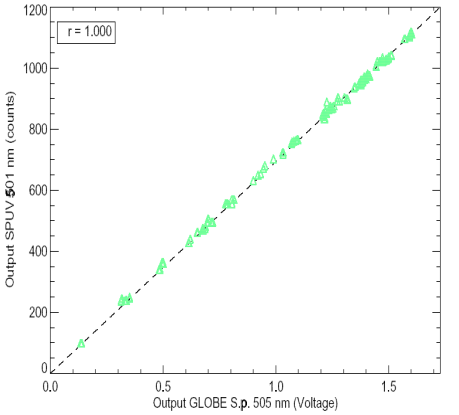

Figure 5.3. Correlation of direct output of GLOBE Sun photometer and SPUV.

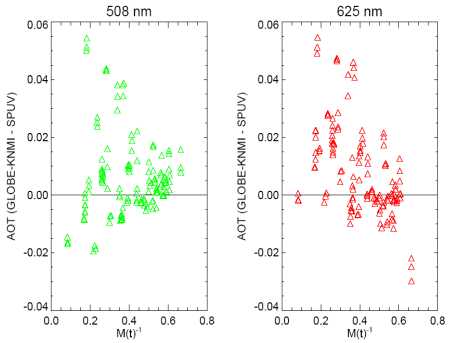

Figure 5.4. $M(t)^{-1}$ dependence of the difference between GLOBE and SPUV AOT.

In order to investigate the nature of the scatter, the differences between coincident GLOBE and SPUV AOT measurements are put in a histogram with bin size 0.006. If the scatter is due to noise, the histogram is expected follow the shape of a Gaussian distribution function and therefore, a Gaussian distribution function is fit to the data. The center of the peak should be at zero in the case that there are no systematic differences between the measurements. The histograms and Gaussian fits are shown in Figure 5.5. The Gaussian fits match the data well in both histograms. The Gaussian curves are both centered at 0.00, suggesting that systematic errors are minor. The $e^{-½}$ halfwidth is the standard deviation (σ), that relates to the uncertainties on GLOBE and SPUV Sun photometer AOT values according to,

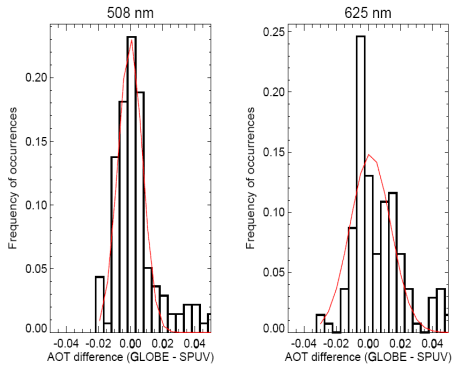

Figure 5.5. Histogram of GLOBE and SPUV AOT difference (nm = 138).

$$\sigma = \sqrt{\left(\sigma_{\tau_a G}\right)^2 + \left(\sigma_{\tau_a S}\right)^2}\ , \qquad \text{(Eq. 5.1)}$$

where $\sigma_{\tau a,G}$ and $\sigma_{\tau a,S}$ represent the uncertainties in GLOBE and SPUV AOT measurements. The standard deviation in SPUV AOT, $\sigma_{\tau a,S}$, is caused by the uncertainty in SPUV output (counts), the

uncertainty in the SPUV extraterrestrial constants and uncertainties introduced at the interpolation. The uncertainty in AOT due to uncertainties in number of counts is negligible (< 0.001 AOT). The uncertainty in SPUV AOT is determined by the uncertainty in the extraterrestrial constants and is smaller than 0.003 AOT. The uncertainty in AOT from the interpolation method is estimated to be smaller than 0.001. Since σ is 0.008 (508 nm) and 0.013 (625 nm) and the errors add quadratically, $\sigma_{\tau a,S}$ in Eq. 5.1 is neglected and σ is used as a direct measure and upper limit for the uncertainty in AOT arising from the comparison with SPUV. The results from the GLOBE - SPUV comparison are summarized in Table 5.2. The offset is the location of the peak of the Gaussian fit and σ is the standard deviation from the Gaussian-analysis. The mean difference (Δ) is also listed in Table 5.2, as well as the standard deviation (σ_Δ) on the mean difference. The maximum of σ and σ_Δ is taken as an upper limit of the uncertainty in AOT. The results in Table 5.2 show that GLOBE and SPUV compare very well and that the uncertainty associated with AOT measurements is smaller than 0.02 AOT, consistent with the result of the theoretical error analysis in section 4.3.

Channel	*r*	offset	σ	Δ	σ_Δ
508 nm	0.97	-0.0002	0.008	-0.006	0.014
625 nm	0.96	-0.001	0.013	-0.007	0.016

Table 5.2. Summary results GLOBE – SPUV comparison.

There are several indications that better determination of the extraterrestrial constants of RG2-047 will lead better results. Until further calibration, the precision of GLOBE AOT measurements is estimated at 0.02 AOT. There is a small offset in both channels of about 0.015 AOT, suggesting systematic errors, which are also expected to improve with new calibration. Since further calibration of RG2-047 may improve the accuracy and precision of the RG2-047 AOT measurements, the 0.02 AOT precision is regarded an upper limit for the precision rather than the maximum attainable precision.

5.2 Validation of GLOBE AOT measurements by undergraduate students with AERONET AOT measurements.

In order to check the quality of AOT measurements with a GLOBE Sun photometer done by undergraduate students, AOT measurements from February 2002 – July 2003 with a GLOBE Sun photometer (RGK-206) from "Christelijk College De Populier'' (latitude = 52.05° North, longitude = 4.16° East), sited in The Hague, are compared to CIMEL Sun photometer AOT measurements from TNO-FEL (latitude = 52.11 North, longitude = 4.33 East), that is part of the world wide aerosol monitoring network Aerosol Robotic Network (AERONET). The CIMEL Sun photometer measures Solar radiance at 440 nm, 675 nm, 870 nm and 1020 nm at TNO-FEL, about three kilometers from ''De Populier''. The AERONET data follows the Ångström relation well and therefore the interpolation of AERONET AOT to 508 nm and 625 nm is done exponentially using the 440 nm and 675 nm channels.

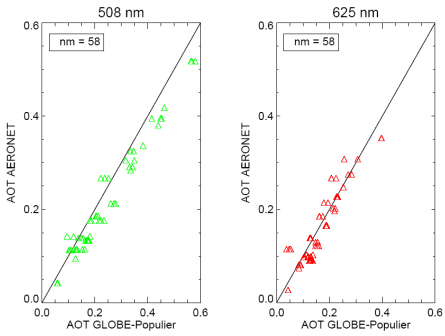

Figure 5.6. Correlation between GLOBE AOT and AERONET AOT at 508 nm and 625 nm.

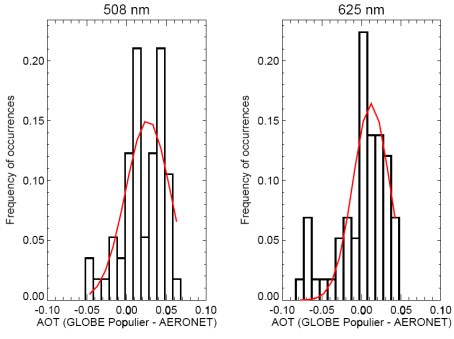

Figure 5.7. Histogram of GLOBE and AERONET AOT differences (nm = 141).

The coincident measurements, done within 10 minutes, for GLOBE and AERONET are shown in Figure 5.6. The correlation coefficients are 0.98 (508 nm) and 0.93 (625 nm). The time criterion is important in the comparison, since aerosol concentrations is variable. A time criterion of 30 minutes instead of 10 leads to r = 0.94 and 0.86. Both channels scatters round the $y = x$ line, the GLOBE measurements at 508 nm seem to be systematically low. In the same sense as in Figure 5.5, a histogram of AOT differences between GLOBE and AERONET coincident measurements is made, with bin size 0.01. The result is shown in Figure 5.7. In both figures, the Gaussian curve matches the data well, except for the right tail, which is not present. This suggests that there is a systematic effect present. Figure 5.8 shows the difference between GLOBE and AERONET AOT as a function of $M(t)^{-1}$. Since there is no distinct linear relation, a systematic error cannot be ascribed to wrong values for the calibration constants.

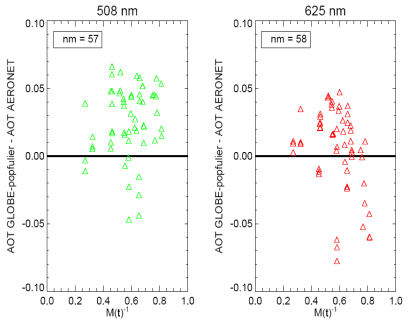

Figure 5.8. $M(t)^{-1}$ dependence of the difference between GLOBE AOT and AERONET AOT.

The $e^{-½}$ halfwidths are 0.03 AOT (508 nm) and 0.02 AOT (625). These relate to the uncertainties in GLOBE and AERONET AOT according to Eq. 5.1, where $\sigma_{\tau a,S}$ should be replaced by $\sigma_{\tau a,A}$, which represents the uncertainty in AERONET AOT. This number is composed from the relative uncertainty in AERONET AOT at 440 nm and 675 nm, which is smaller than 0.006 AOT, and the uncertainty from the interpolation, which is 0.003 AOT. Consequently, the uncertainty in AERONET AOT is smaller than 0.007 AOT. Since σ is 0.03 AOT (508 nm) and 0.02 AOT (625 nm), $\sigma_{\tau a,A}$ is neglected and σ is taken as a measure for the uncertainty in AOT arising from the comparison with AERONET. The results from the GLOBE - AERONET comparison are summarized in Table 5.3. The location of the peak of the Gaussian fit is taken as yhe offset and σ is the standard deviation from the Gaussian-analysis. The mean difference (Δ) is also listed in Table 5.3, as well as the standard deviation (σ_Δ) on the mean difference. The precision of GLOBE AOT measurements from this analysis is 0.03 AOT. Since ''De Populier'' and TNO-FEL are 3 km apart, AOT gradients may cause part of the scatter and this precision is regarded as an upper limit.

Channel	r	offset	σ	Δ	σ_{md}
508 nm	0.98	0.03	0.03	0.03	0.03
625 nm	0.93	0.01	0.02	0.006	0.03

Table 5.3. Summary results GLOBE – AERONET comparison.

The precision of GLOBE student AOT measurements is estimated at 0.03 AOT for The Hague with small offsets for both channels. ''De Populier'' is the only school measuring AOT close to a professional measuring site. Assuming that ''De Populier'' is representative for all GLOBE schools, meaning that students from other schools are able to measure AOT as accurately as the Populier students, we use de precision obtained by the Populier – AERONET comparison, which is 0.03 AOT, for all the GLOBE schools in the project. However, it will be necessary to keep comparing results of The Hague measurements with AERONET measurements. Furthermore, schools close to KNMI have joined the GLOBE Aerosol Monitoring Project, so that measurements of these schools can be compared with measurements at KNMI, in order to make an even better estimation of the accuracy and precision of GLOBE student AOT measurements.

5.3 Conclusion

The first conclusion of this section is that a GLOBE Sun photometer is able to measure AOT with a precision better than 0.02 AOT. The main contribution to this uncertainty comes from the

extraterrestrial constants. New calibration results are expected since the instrument is expected to go to the Swiss atmospheric observation station at Jungfraujoch (elevation = 3500 m) for calibration. The second conclusion of this section is that undergraduate students are able to measure AOT with the GLOBE Sun photometer with a precision better than 0.03 AOT. This result is obtained from a comparison from one key-school with a professional instrument, and the assumption that other schools will obtain similar results. The validity of this assumption can be checked soon since a new school at Bilthoven, close to De Bilt will join the project which enables a comparison between this school and measurements at KNMI.

6 MODIS AOT Validation

Several satellites carrying various instruments circle around the earth monitoring atmospheric parameters derived from measured radiance reflected by the earth. Instruments on geostationary satellites view a fixed area on the globe. On the other hand, instruments placed on polar satellites, such as MODIS (Moderate Resolution Imaging Spectroradiometer), SCIAMACHY (Scanning Imaging Absorption Spectrometer for Atmospheric Cartography) and OMI (Ozone Monitoring Instrument), obtain global coverage every one (OMI) to six (SCIAMACHY) days. Validation with ground-based measurements is essential to monitor the accuracy and precision of measurement from these instruments. The goal of the GLOBE Aerosol Monitoring Project in the Netherlands is to extend and improve validation of aerosol optical thickness measurements by SCIAMACHY and OMI, which are instruments that are (partly) developed in the Netherlands. Since the OMI launch is due January 2004 and SCIAMACHY is still in the commissioning phase, the GLOBE Aerosol Monitoring school network is used to validate MODIS aerosol optical thickness measurements.

6.1 The MODIS instrument

There are two MODIS instruments, one aboard NASA's satellite Terra, launched December 18, 1999, and the other is aboard NASA's satellite Aqua, launched May 4, 2002. Terra passes from north to south across the equator in the morning, while Aqua passes south to north over the equator in the afternoon. In this work the MODIS instrument on Terra is validated. Validation of MODIS on Aqua is planned for future work. The MODIS instrument measures radiances in 36 spectral bands between 0.4 μm and 14.4 μm. Aerosol optical thickness is measured at 0.470 μm and 0.660 μm. The spatial resolution of MODIS is 10×10 km^2. The EOS orbit at 705 km and a 55° viewing angle gives a 2330 km swath and provides global coverage every one to two days. For more detail on the MODIS instrument see [*Kaufman and Tanré*, 1998].

6.2 MODIS Algorithm

The MODIS instrument measures the radiance that is reflected by the earth. The MODIS algorithm is based on the look-up table (LUT) approach. Following this approach, radiance measurements by MODIS are compared to pre-computed (simulated) radiances for different values of atmospheric and surface parameters. The pre-computed radiance that matches the measured radiance best is used to retrieve the desired aerosol parameters, a.o. aerosol optical thickness (τ_a). The geometry of the MODIS measurement is shown in Figure 6.1. The solar zenith angle, θ_0, the MODIS viewing agle, θ, the azimuth of the scattered radiation from the solar beam, ϕ-ϕ_0, and the scattering angle, Θ, are indicated. The angle between the 'In' and 'Out' beam is π - Θ, since the Θ

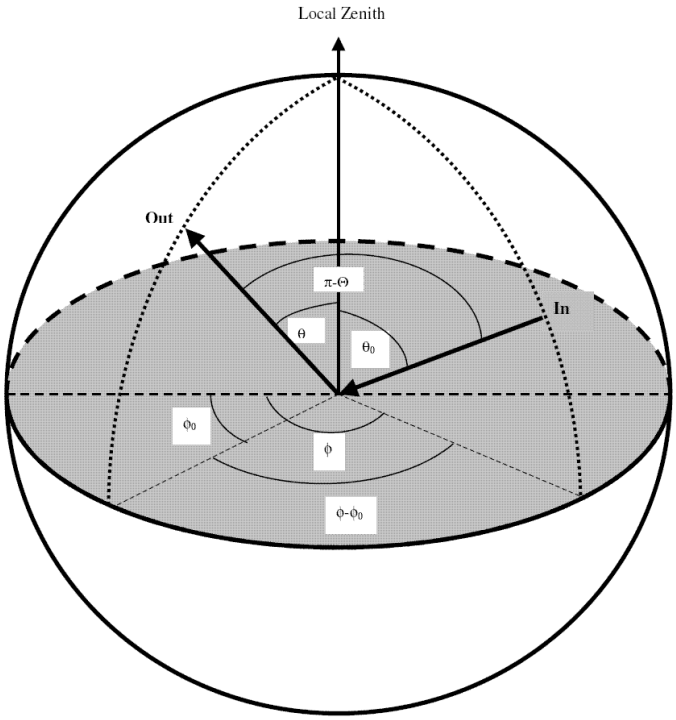

Figure 6.1. Geometry of the MODIS measurement

is defined in a way that a zero scattering angle represents forward scattering and a scattering angle of π radains represents backscattering. All the angles are defined at the top of the atmosphere (TOA).

Figure 6.2 shows the reflected radiance that is detected by MODIS. The radiance detected by MODIS is composed by radiance scattered by the atmosphere and radiance reflected by the earth's surface. The scattered radiance is called the path radiance. The radiance detected by MODIS, I_{TOA}, can be written in flux units as the sum of the path radiance and the radiance reflected from the earth's surface as a function of θ, θ_0, and ϕ [*Kaufman and Tanré*, 1998],

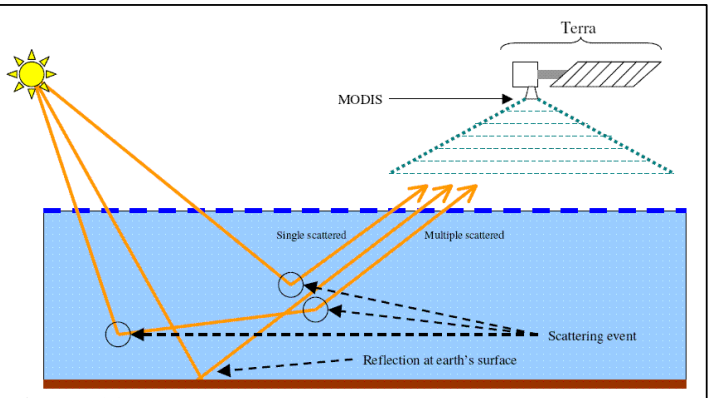

Figure 6.2.

$$\pi I_{TOA}(\theta,\theta_0,\phi-\phi_0)=\mu_0 F_0 R_a(\theta,\theta_0,\phi-\phi_0)+\mu_0 F_0 F_d(\theta_0)T(\theta)\frac{R_s(\theta,\theta_0,\phi-\phi_0)}{1-sR'}, \quad \text{(Eq. 6.1)}$$

where μ_0 is the cosine of the solar nadir angle, F_0 is the extraterrestrial solar flux, R_a is the path reflectance, F_d is the Sun normalized downward flux for zero surface reflectance, $T(\theta)$ is the upward total transmission into the direction of the satellite, $R_s(\theta,\theta_0,\phi\text{-}\phi_0)$ is the surface bi-directional reflectance, s is the atmospheric backscattering ratio and R_s is the surface reflectance averaged over the field of view. The dependence on aerosol is present in R_a. In principle, there is a dependence on τ_a in the second term on the right hand side of Eq. 6.1, but for small surface reflectance, at which useful retrieval is done, they are neglected. In the single scattering approximation, it is assumed that the intensity of multiple scattered radiance is negligible compared to the intensity of single scattered radiance. The path radiance in reflectance units may then be written [*Kaufman and Tanré*, 1998],

$$R_a(\theta,\theta_0,\phi-\phi_0)=R_m(\theta,\theta_0,\phi-\phi_0)+\omega_0\tau_a P_a(\Theta)/4\mu\mu_0\,, \quad \text{(Eq. 6.3)}$$

where R_m is the path radiance due to molecular scattering, τ_a is the aerosol optical thickness, $P(\Theta)$ is the aerosol scattering phase function, μ is the cosine of the viewing angle and ω is the single scattering albedo, which is defined as the ratio of the scattering coefficient to the extinction (scattering and absorption) coefficient in the form,

$$\omega_0=\frac{\beta_s}{\beta_e}. \quad \text{(Eq. 6.2)}$$

The MODIS algorithm, using Eq. 6.1 and Eq. 6.2, is schematically depicted in Figure 6.3 and the steps are described below.

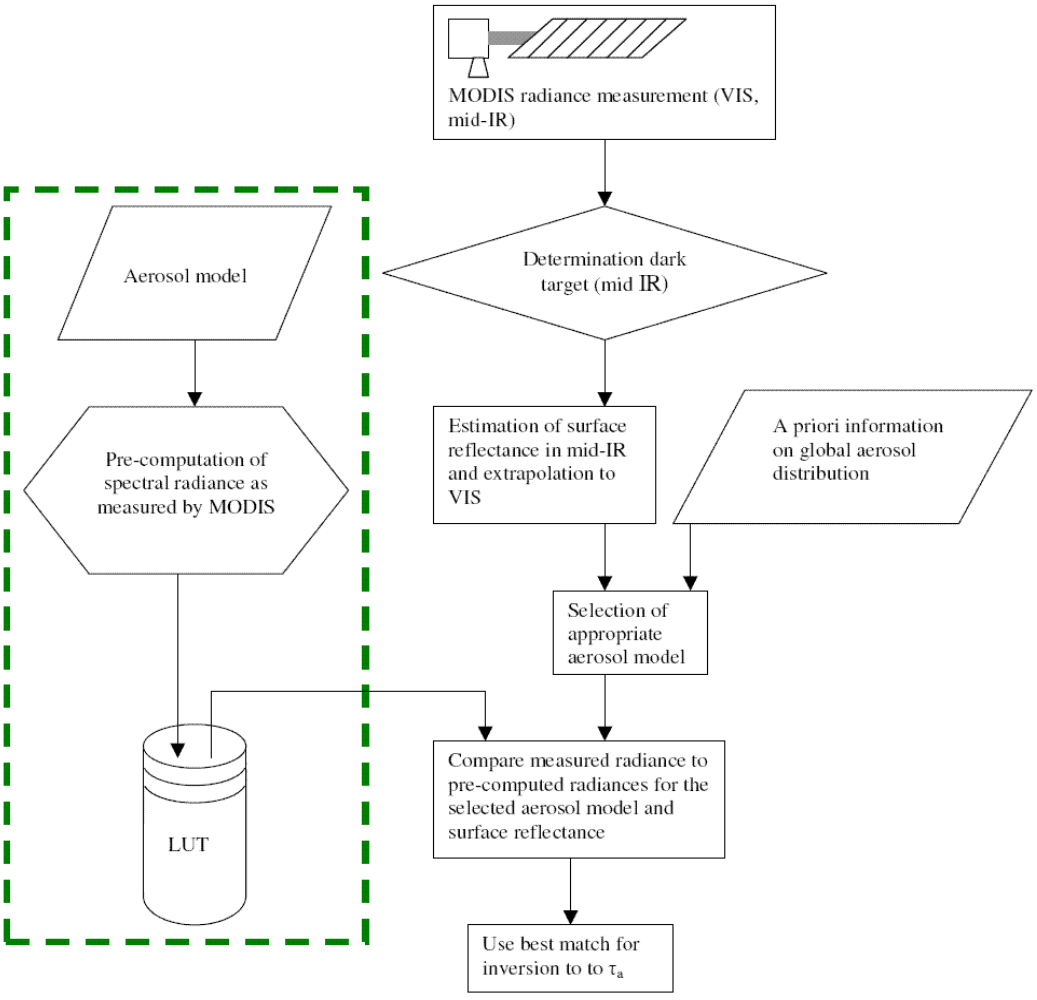

Figure 6.3. MODIS measurement method.

0. Beforehand, MODIS measured radiances are pre-computed for several values of atmospheric and surface parameters and the results are stored in so-called look-up tables. This process is indicated by the green rectangle. Aerosol models, describing ω_0, $P(\Theta)$, τ_a and other aerosol parameters such as vertical distribution, are used in the computation.
1. In a 10x10 km^2 grid box, cloud-free pixels are first selected using the MODIS cloud mask. The cloud mask indicates a cloudy or clear pixel of 1x1 km^2 resolution.
2. Since the contribution of the path radiance to I_{TOA} is higher for small surface reflectance, the errors in deriving τ_a are smaller for small surface reflectance. Therefore, pixels with high reflectivity, caused by for example snow, are taken out of the analysis. This is the so-called dark target approach. The determination of dark targets is done in the mid-IR, at 2.1 and 3.8 μm, since the atmosphere is more transparent at these wavelengths.
3. The reflectance, R_s, is measured with the mid-IR channels, at 2.1 and 3.8 μm. The results are extrapolated to the VIS channels based on an empirical function [*Kaufman and Tanré*, 1998] to estimate $R_s(\theta,\theta_0,\phi\text{-}\phi_0)$ at 470 and 660 nm.
4. The measuring method requires assumption on aerosol type. This is done using a priori information on global aerosol type distribution. The aerosol type is used to select the appropriate aerosol model that describes the aerosol size distribution, refractive index, single scattering albedo, the aerosol scattering phase function and the vertical distribution of the aerosol loading.

5. The measured radiance is compared to the pre-computed radiances in the look-up tables with the appropriate aerosol model and surface reflectance. The pre-computed radiance that matches the measured radiance best (least squares) is obtained by interpolation between radiances in the look-up tables.
6. The best match is used to derive aerosol optical thickness, volume concentration and spectral radiative forcing.

The main error sources are the reflectivity of the earth surface and the aerosol model. Errors in AOT are estimated to be $\sigma_\tau = \pm 0.05 \pm 0.2\tau_a$ ($\approx$ 100% error at τ_a 0.05).

6.3 Validation results

Since the MODIS instrument measures AOT at 470 nm and 660 nm, GLOBE measurements at 508 nm and 625 nm should be extrapolated to the MODIS wavelengths. This is done by using the Ångström relation in Eq. 2.1. One way to determine α is from the spectral dependence of AOT from the two GLOBE channels. However, this would mean that α would depend on the calibration constants of both the GLOBE channels. Since the calibration constants are the main error source in the GLOBE AOT results this would increase the potential error in α. Therefore, an a priori α is taken, until GLOBE calibration results are improved. For measurements at KNMI α is taken from the mean value of five years of SPUV measurements. For GLOBE measurements α should also be the climatological mean at the measuring site. Since these values are not known, the mean α at De Bilt is taken as a preliminary value for α for all GLOBE schools. This may introduce systematic errors, until the Ångström coefficients are known for every measuring site. The mean value of α at De Bilt is 1.398 ± 0.60 [*Stammes, private comm.*, 2003], [*Stammes and Henzing,* 2000]. The sensitivity of the extrapolation to α is obtained by differentiating Eq. 2.1 with respect to α,

$$\frac{\partial \tau(\lambda)}{\partial \alpha} = -\tau(\lambda_0) \cdot \ln\left(\frac{\lambda}{\lambda_0}\right) \cdot \left(\frac{\lambda}{\lambda_0}\right)^{-\alpha} . \qquad \text{(Eq. 6.4)}$$

Since τ(508) is larger than τ(625) and for the extrapolation from 508 to 470 and from 625 to 660 nm, λ/λ_0 is approximately the same, the extrapolation to 470 nm is most sensitive to errors in α. The sensitivity of the extrapolation to 470 nm to α is shown for De Bilt in Figure 6.4. The slope represents the sensitivity of the extrapolated value for α. The dependence on α is very weak and a linear fit represents the data well. The uncertainty in the extrapolated AOT at 470 and 660 nm arising from the uncertainty in the Ångström coefficient is 0.024 AOT for De Bilt. Systematic errors arising from a systematically low or high value of α for GLOBE measuring sites are estimated to be less than 0.02 AOT, based on a maximum error in α of 0.5. The total uncertainty for GLOBE AOT at MODIS wavelength becomes

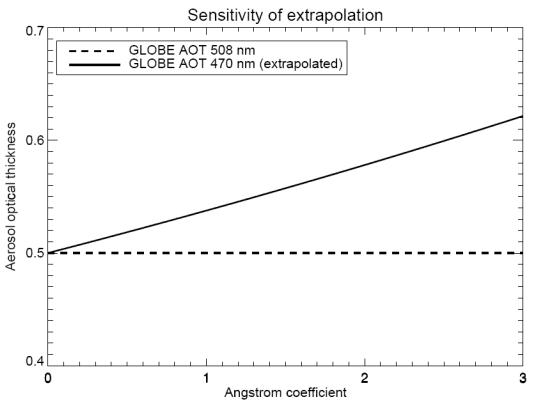

Figure 6.4. Sensitivity of the extrapolation of GLOBE AOT at 508 nm to MODIS 470 nm.

$$\sigma_{G\to M} = \sqrt{(\sigma_G)^2 + (\sigma_{ext})^2 + (\sigma_\alpha)^2} , \qquad \text{Eq. 6.5}$$

where σ_G is the uncertainty at the GLOBE wavelength from the comparison with AERONET, which is estimated 0.03 AOT, σ_{ext} is the uncertainty arising from the extrapolation and $\sigma_{G\to M}$ is the uncertainty at the MODIS wavelength, taken from the MODIS data file.

From the nine schools, measurements from only three schools can be used for validation. A reason for that is that 5 schools have joined the project in June 2003, and schools have shown to need a certain start-up time. Furthermore, the data-access at the GLOBE site gives problems, and probably unprocessed data is still at the schools. Since the problems with the GLOBE site should soon be solved, these data are expected to be processed soon. The schools currently involved in the validation effort are "Christelijk college De Populier'' at The Hague (31 matches with MODIS), "Bernard Nieuwentijt college'' at Amsterdam and Marken (5 matches with MODIS at Amsterdam, 18 matches at Marken) and "Mozaiek'' college (2 matches with MODIS). The Marken site is from a student from "Bernard Nieuwentijt college'' who took the Sun photometer home during the holidays to measure AOT in the summer of 2003. A GLOBE measurement is regarded as a match with MODIS if a MODIS measurement was done within 2 hours from the GLOBE measurement. The number of matches is expected to be smaller than the number of GLOBE measurements. This is because:

1. MODIS does not have global coverage every day.
2. MODIS could not always measure due to clouds or snow.
3. MODIS only measures once a day, so when there is more than one GLOBE measurement at the same day, the one closest in time to the MODIS measurement is used for validation.

Figures 6.5 till 6.9 show the coincident measurements of MODIS and GLOBE for KNMI, the three schools and the measurements at Marken. The measurements are performed between September 2002 and September 2003. Every MODIS measurements has a cloud fraction associated with it between 0% and 100%, which indicates the amount of the 1x1 km^2 sub-pixel covered by clouds. All pixels with cloud fraction between 0% and 100% are included in the analysis and anomalous AOT values can always be checked on cloud fraction. MODIS compares relatively well with GLOBE measurements at KNMI. Sometimes, GLOBE AOT is higher, sometimes MODIS AOT is higher. This indicates that the differences are mainly due to noise. However, relative errors may be high due to the low AOT values. The MODIS values for the comparison with The Hague seem to follow the GLOBE measurements, that is if GLOBE is high (or low), MODIS is high (or low) too, but compared to GLOBE MODIS seems to be systematically high. Furthermore, the MODIS measurements show a larger variation in AOT values. The comparison with Amsterdam shows approximately the same result as for De Bilt, that is relatively low AOT values and sometimes higher MODIS value, sometimes a higher GLOBE value, although MODIS seems to be somewhat high for the 470 nm channel. The MODIS comparison with Marken in Figure 6.8 shows approximately the same behavior as in Figure 6.6, there is some agreement but MODIS AOT is systematically higher than GLOBE AOT. MODIS shows good agreement with GLOBE at Arnhem in Figure 6.9, but there are only three comparisons.

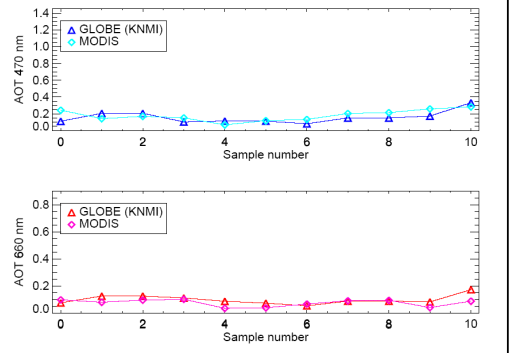

Figure 6.5. KNMI (De Bilt)

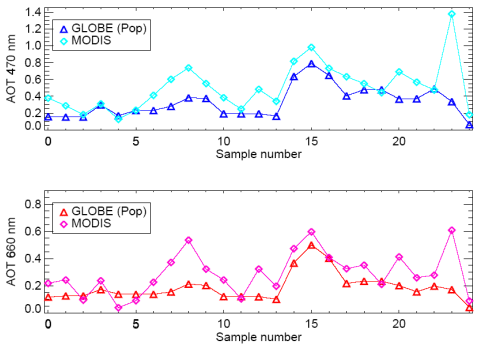

Figure 6.6. Populier (The Hague)

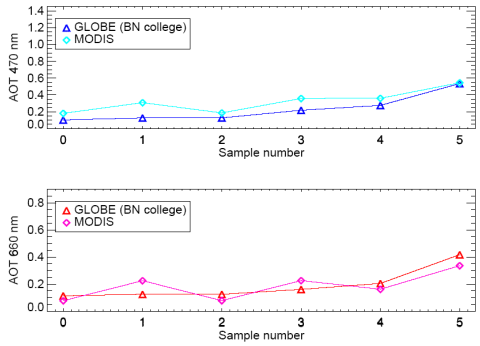

Figure 6.7. BN college (Amsterdam)

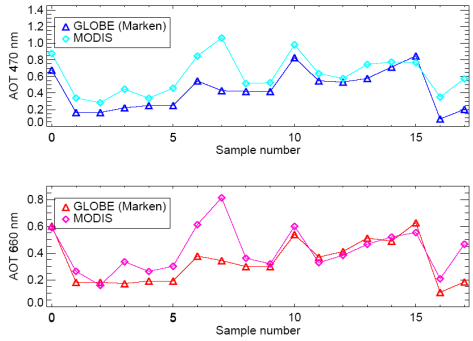

Figure 6.8. Marken

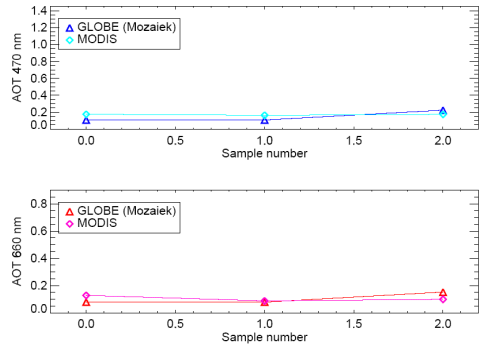

Figure 6.9. Mozaik college (Arnhem)

Scatter plots for De Bilt, The Hague and Marken are shown in Figures 6.10 tm 6.12. For De Bilt the 470 nm channels scatters round the $y = x$ line, but the 660 nm channels shows a small offset, indicating that MODIS measures systematically lower AOT than MODIS. However, the differences are within the estimated uncertainty of about 0.1 AOT. For both The Hague and Amsterdam, in Figures 6.11 and 6.12, MODIS AOT values are systematically high for both the 470 and 660 nm channels. This indicates that, at these locations, MODIS overestimates AOT. This is ascribed to the fact that Marken and The Hague are both coastal regions, which will be discussed below.

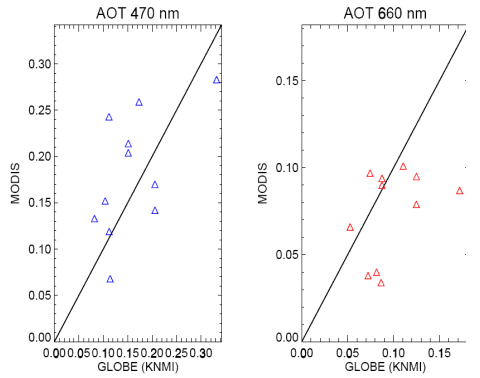

Figure 6.10. Scatterplot for MODIS comparison at De Bilt.

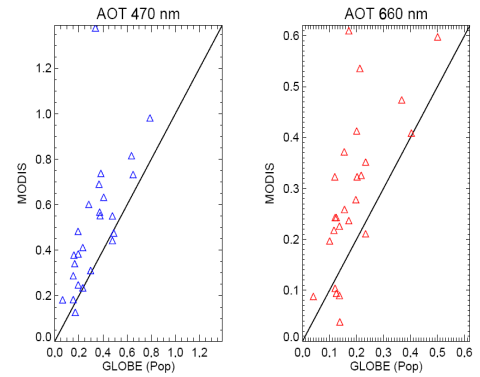

Figure 6.11. Scatterplot for MODIS comparison at The Hague.

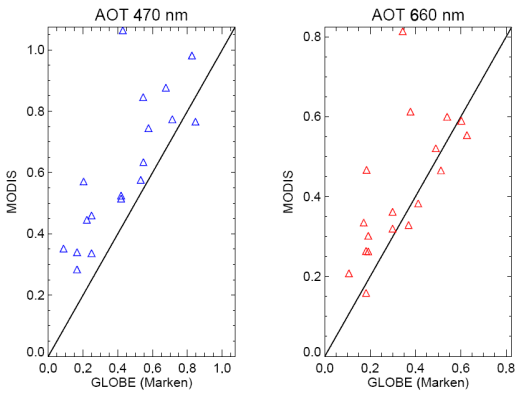

Figure 6.12. Scatterplot for MODIS comparison at Marken.

	$\|\Delta t\|$	#matches	r_{470}	r_{660}	Δ_{470}	$\sigma_{\Delta,470}$	Δ_{660}	$\sigma_{\Delta,660}$
KNMI	74 min	11	0.57	0.40	-0.02	0.06	0.02	0.03
Populier	69 min	31	0.66	0.67	-0.18	0.21	-0.10	0.12
Marken	89 min	18	0.79	0.67	-0.18	0.15	-0.08	0.14

Table 6.1. Results of analysis from MODIS validation with GLOBE measurements.

The mean absolute time difference, $|\Delta t|$, correlation coefficients r, mean differences Δ, which may indicate the presence of systematic errors and standard deviation of the mean difference σ_Δ, which is a measure for the scatter, are shown in Table 6.1. The mean absolute time difference is larger than 60 minutes for all three comparisons, which is large, considering the variability of aerosol. The correlation coefficients for the KNMI data set are very small. However, the data set is small to draw a useful conclusion from the bad correlation coefficients. The mean difference and standard deviation are relatively small, which indicates good agreement. The mean difference is smaller than the combined uncertainty from Eq. 6.5, which is about 0.07 AOT. This indicates that systematic errors are minor. The correlation coefficients for The Hague are better than the KNMI coefficients, but still relatively low. The correlation coefficients are very much influenced by one outlier, at sample nr. 23. Without this outlier, the values for r would be 0.84 (470 nm) and 0.73 (660 nm). This is somewhat better than the values in Table 6.1. The mean difference indicates that MODIS is systematically higher than GLOBE and the scatter is relatively large. The results for Marken are comparable to the values for The Hague. There again is one outlier that influences the value of r. Without this outlier the r-values are 0.90 (470 nm) and 0.82 (660 nm), which is better than the values in Table 6.1. MODIS is systematically high and the scatter is relatively large.

A MODIS validation campaign by *Chu et al* [2002] has shown that MODIS has difficulties with estimating AOT for pixels that are partly over water.. A reason for that may be that the empirical relation that is used to determine the surface albedo at 470 and 660 nm is valid only for land surfaces. The MODIS measurements seem to agree somewhat better with the KNMI measurements than with the The Hague and Marken measurements. In order to check if MODIS overestimates AOT at The Hague and Marken pixels, which are both partly over water, the measurements from The Hague and Marken are compared to the neighboring pixel. on the land side. Additional errors may be introduced since the measurements are no longer collocated. The results of the comparison of The Hague and Marken with the neighboring pixel are shown in the Figures 6.14 and 6.15. Both measurements from The Hague and Marken compare much better with the neighboring pixel, which is over land, than with the actual pixel, which is partly over water. This indicates that the MODIS instrument has troubles measuring AOT at these pixels., which is in agreement with other validation campaigns with *Chu et al*

[2002]. The MODIS results at 470 nm are still systematically high compared to GLOBE. Since this is not the case at 660 nm this may be ascribed to systematic errors arising from a systematically wrong value for the Ångström coefficient. Note that there are more matches for these MOLDIS pixels than for the coastal MODIS pixels. This is because the MODIS algorithm sometimes rejects measurements that are partly over water.

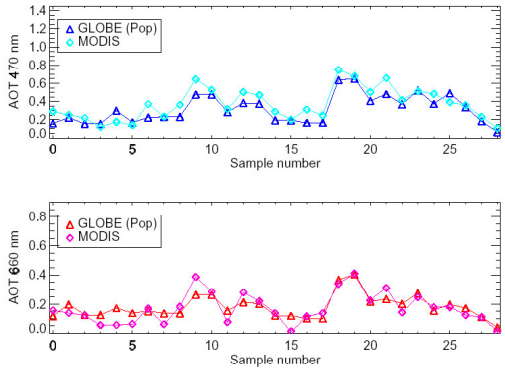

Figure 6.14. GLOBE The Hague comparison with neighboring (East) MODIS pixel

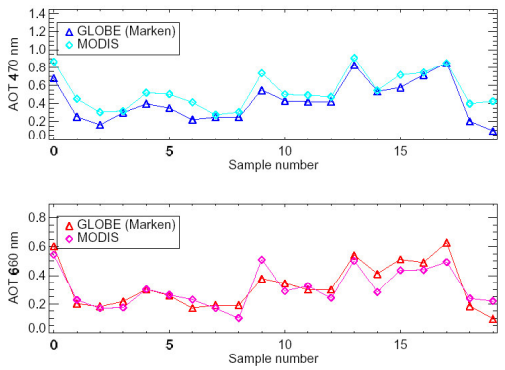

Figure 6.15. GLOBE Marken comparison with neighboring (West) MODIS pixel

It is shown in section 5.2 that the time difference between the collocated measurements can be of large influence on the results of the comparison, due to the variability of aerosol concentrations. When the time criterion is set to 10 minutes, for The Hague five matches are found and for the other measuring sites no match is found. Figure 6.16 shows the coincident measurements for The Hague and MODIS (neighboring pixel) within 10 minutes. The measurements agree much better than the result in Figure 6.14, as expected. The data set is too small to make a serious quantative estimate of the level of agreement of the GLOBE and MODIS measurements. In order to show how the differences relate to the estimated uncertainties in AOT, Figure 6.17 shows the difference for the coincident GLOBE and MODIS measurements at The Hague for the neighboring pixel with a 10 minutes time criterion. The errors using Eq. 6.5 are plotted as error bars. The results are within the estimated uncertainty. The measurements are checked for MODIS cloud fraction and GLOBE metadata, and this gives no reason to reject points. Since wind can take aerosol loadings to neighboring pixels, we should look at wind speed and direction and coupling to the time criterion for every pixel in order to improve the results. This is something that should be done in future work.

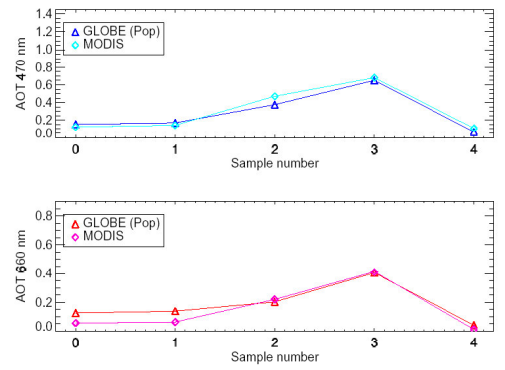

Figure 6.16.

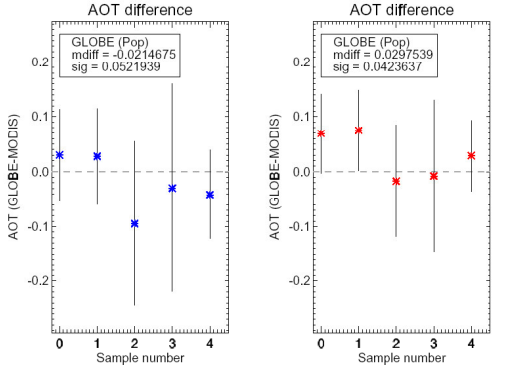

Figure 6.17.

6.4 Conclusion

GLOBE highschool student aerosol optical thickness measurements with the GLOBE Sun photometer are used to validate MODIS AOT measurements. The results compare reasonably well even when a mean time difference criterion of 2 hours is used. When the time criterion is set at 10 minutes, the results compare remarkably well. This shows that it is important to choose an appropriate time criterion for validation since it is essential that GLOBE and MODIS measure the same air sample. The 10 minutes time criterion only left 5 comparisons at The Hague. In order to make a quantative statement, more comparisons are needed. For coastal pixels, MODIS AOT results are relatively high compared to GLOBE AOT results. The comparisons of costal pixels improve significantly when the GLOBE measurements are compared to the neighboring (land-) pixel instead of the costal pixel. This is a strong indication that MODIS overestimates AOT at pixels that are partly over water. The results confirm the high potential for satellite instrument validation of the GLOBE school network, since similar results were achieved by validation campaigns with professional Sun photometers.

To improve the validation of satellite measurements with the Dutch GLOBE school network, more measurements are necessary. When the new GLOBE schools start doing measurements on a routine basis and new schools have joined the project the validation can extend to a larger scale and results can be better analyzed by improved statistics. GLOBE measurements within 10 minutes of the satellite overpass time are very useful since the time difference between GLOBE and satellite instrument measurements has shown to have great impact on the validation results. A relatively quick and simple action to extend the validation is comparing the GLOBE data with MODIS on Aqua. Furthermore, the current GLOBE school measurements can be used to validate SCIAMACHY AOT measurements when SCIAMACHY data is released.

7 Conclusion and Outlook

In this report the contribution of the GLOBE Aerosol Monitoring school network to validation of aerosol measurements by satellite instruments was investigated. There is a need for aerosol monitoring since aerosols influence the climate system of the Earth. The GLOBE school network provides a network of ground based AOT measurements with a spatial resolution which is not achieved by professional instruments. Therefore the GLOBE school network has high potential for validation of satellite instrument AOT measurements. The GLOBE measurements are done with the broadband LED-based GLOBE Sun photometer. Solar radiance measurements are done with two LED's, one in the green wavelength range with effective wavelength 508 nm and the other in the red wavelength regime range with effective wavelength 625 nm. The effective wavelength is defined at TOA, in order to have a effective wavelength that is independent of conditions at the measuring location. This may leads to errors whose extend is still to be investigated. The measurement method of the GLOBE Sun photometer is based on the monochromatic BBL law. Errors arising from the large bandwith of the GLOBE Sun photometer are significant for Solar zenith angles larger than 80°. Therefore, measurements at Solar zenith angles larger than 80° are rejected. Since these errors depend on AOT and Ångström coefficient the extend of these errors should also be investigated for a range of AOT values and Ångström coefficients in future work. Effects arising from different vertical distributions of attenuators in the atmosphere and refraction in the atmosphere are negligible for measurements at Solar zenith angles smaller than 80°.

In order to be able to accurately translate Solar radiance measurements to AOT the instrument's extraterrestrial constants of the two channels must be known with a high degree of accuracy. The degree of accuracy at which the extraterrestrial constant of the instrument used at KNMI, the so-called reference instrument, is estimated to be 50 mV, which is not yet satisfactory. These constants are essential to the project since all other instruments are calibrated relative to this one reference instrument. Nevertheless, the algorithm that was developed to calculate AOT from GLOBE Solar radiance measurements gives reliable results. In order to account for the LEDs' large bandwiths, effective values for Rayleigh scattering and ozone absorption are used. The results of the algorithm compare well with the on-line GLOBE algorithm. However, the GLOBE algorithm does not include ozone absorption and therefore overestimates AOT. When ozone is not taken into account there are some very small differences due to different relative air mass calculations and different values for the effective Raylegh optical thickness.

The average uncertainty (or precision) associated with AOT measurements by the GLOBE Sun photometer is estimated at 0.02 AOT from a theoretical error analysis. The main cause of this uncertainty is the uncertainty in the extraterrestrial constants, which again illustrates the need to improve the accuracy of these values. Uncertainty in signal voltage and measurement time contributes little, and uncertainty in pressure and ozone column is negligible. GLOBE Sun photometer measurements also show to attain in practice this precision of 0.02 AOT in a comparison with a professional instrument at KNMI. GLOBE students show to attain a 0.03 AOT precision by a comparison with the AERONET instrument at TNO-FEL in The Hague. Since the GLOBE and AERONET measuring locations are 3 km apart, this 0.03 AOT is regarded an upper limit. Schools close to KNMI have joined the project so that GLOBE measurements at KNMI and at GLOBE schools can directly be compared, in order to get a better estimate of the precision of GLOBE student AOT measurements.

The GLOBE AOT precision of 0.03 AOT is encouraging for the validation, since this is better precision than the reported MODIS AOT (< 0.05 AOT) and of the order of magnitude of AERONET AOT (0.01 – 0.02 AOT). A somewhat larger uncertainty than AERONET measurements is not a large problem when there are enough measurements so that statistics can be applied and errors will cancel. MODIS AOT results compare well with GLOBE AOT results. On the whole MODIS vaslues seem to be somewhat larger than GLOBE values. Comparisons of MODIS with GLOBE at coastal regions have shown that MODIS overestimates AOT at coastal regions. This is probably due to erroneous

estimation of the surface reflectance by the MODIS algorithm. It is essential for high quality validation that GLOBE and MODIS measurements occur within 10 minutes, since validation results deteriorate dramatically when time differences get up to 30 minutes or more. This is a very important result since it illustrates the need for GLOBE schools to frequently check satellite overpass predictors.

Outlook

The most important work that is to be done is very accurate calibration of the reference instrument at KNMI, RG2-047. This will make AOT results of all the schools in the GLOBE Aerosol Monitoring Project more reliable and may show that errors are currently overestimated. There are plans to take the reference instrument to Jungfraujoch (elevation = 3500 m.) to do a very accurate calibration. Furthermore the extend of errors arising from defining the effective wavelength at TOA and the dependence on AOT and Ångström coefficient of errors arising from the LED's large bandwith should be investigated.

In order to get a even better estimation of the precision at which GLOBE student measure AOT the comparison of "De Populier" with AERONET will be extended with more measurements and possibly with taking into account wind speed and direction with respect to the distance between the measuring locations. Furthermore, future results from the new school at Bilthoven, close to KNMI, will be compared to measurements at KNMI.

With respect to validation activities, one of the most urgent things is using a better value for the Ångström coefficient that is used for extrapolating GLOBE values to MODIS wavelengths. When the renewed calibration of the reference instrument is finished, the Ångström coefficient can be taken directly from the two channel GLOBE AOT measurements. The validation will be extended to MODIS Aqua measurements. This may be of great additional value since the Aqua overpass time is somewhat later than that of Terra, and the amount of collocated measurements within 10 minutes may be significantly larger than for the comparison with Terra, possibly resulting in preliminary quantative validation results. Within a few years the GLOBE school network is supposed to be used on a routine basis for quantitative validation of SCIAMACHY and OMI AOT measurements.

REFERENCES

Allaart, M, P. Valks, R. Van der A, A. Piters, H. Kelder, P. Van Velthoven, Ozone mini-hole observed over Europe, influence of low stratospheric temperature on observations, *Geophys. Res. Lett, 27,* 4089-4092, 2000

Ångström, A. On the atmospheric transmission of Sun radiation and on dust in the air, *Geogr. Ann., 11*, pp.156-166, 1929

Brooks, D.R., F,M. Mims, III, Development of an Inexpensive Handheld LED-Based Sun Photometer for the GLOBE Program, *J. Geophys. Res, 106*, 4733-4740, 2001

Chu, D. A., Y. J. Kaufman, C. Ichoku, L. A. Remer, D. Tanré, B. N. Holben, Validation of MODIS aerosol optical depth retrieval over land, *Geophys. Res. Lett, 27,* Vol. 29, NO. 12, 2002

Haan, S. de, S. Barlag, The use of Near Real Time GPS-IWV for Operational Meteorology and Nowcasting, *J. Meteor. Soc. Jap*., 2003

Hasekamp, O.P., *Retrieval of aerosol properties from multispectral direct Sun measurements*, 1998

Houghton, John T., *The physics of atmospheres*, 2nd edition, Cambridge University press, New York, 1986

Intergovernmental Panel on Climate Change (IPCC). *Climate Change 2001-The Scientific Basis*, Cambridge Univ. Press, Cambridge, 2001

Kaufman, J. Y., D. Tanré, Algorithm for remote sensing of tropospheric aerosols from MODIS, *MODIS Algorithm Theoretical Basis Documents*, 1998

Kaufman, J. Y., D. Tanré, O. Boucher, A satellite view of aerosols in the climate system, *Nature,* VOL 419, 2002

Liou, K.N., *An Introduction to Atmospheric Radiation*, 2nd edition, Academic press, London, 2002

Mims, F.M., III, Sun photometer with light emitting diodes as spectrally selective detectors, *Appl. Opt., 31*, 6965-6967, 1992

Stammes, P., J.S. Henzing, Multispectral Aerosol Optical Thickness at De Bilt, 1997-1999, *J. Aerosol Sci., 31*, S283-S284, 2000

Thomason, L.W., B.M. Herman, J.A. Reagan, The Effect of Atmospheric Attenuators with Structured Vertical Distributions on Air Mass Determinations and Langley Plot Analyses, *J. Atmos. Sci., 40*, 1851-1854, 1983, TR-207, KNMI, De Bilt, 1998

Young, A.T., Air mass and refraction, *Appl. Opt. 33:6*, 1108-1110, 1994

Acknowledgements

Several people contributed to this work, for which I would like to thank them.

First of all I would like to thank Folkert Boersma, my direct supervisor at KNMI. It was the enthusiasm for the project that you put in your first emails and at that first training that brought me to KNMI. You were always ready to solve problems together, or to take a look at another picture of fresh results, or to give another set of comments you had on my report. You contributed not only to the work and report, but also to my motivation.

I would like to thank Wim Vassen, my supervisor at the Vrije Universiteit Amsterdam and Pieternel Levelt from KNMI.

I thank David Brooks from Drexel University, Philadelphia, Marc Allaart and Piet Stammes from KNMI and Marcel Moerman and Gerrit de Leeuw from TNO-FEL for their contributions by providing data and answer questions. I would like to thank Johan de Haan for first corrections to the report.

I would like to thank my parents for their support, both financially and by stimulating me do finish this work in time.

Special thanks goes to Willemijn Homans. Willemijn, thank you for your unconditional believe in me. This I appreciate probably more than you realize. However, you were not reluctant to be critical by asking me questions about statistics that took me more than a day to answer, thereby motivating me to get the theory right. I hope I can do the same for you in the near future since you are not very far from a(nother) graduation yourself.